Hydromechanics of the Koyna-Warna region, India

Inmaculada Durá-Gómez[1] and Pradeep Talwani[1]
(1) Department of Geological Sciences, University of South Carolina, Columbia, South Carolina 29208, U.S.A.
E-mail:talwani@geol.sc.edu

Abstract
Continuous reservoir induced seismicity has been observed in the Koyna-Warna region in western India following the beginning of impoundment of Koyna and Warna Reservoirs in 1961 and 1985 respectively. This seismicity includes 19 events with M≥5.0 which occurred in 7 episodes (I to VII) between 1967 and 2005 at non-repeating hypocentral locations. In this study, we examined the first six episodes. The seismicity occurs by diffusion of pore pressures from the reservoirs to hypocentral locations along a saturated, critically stressed network of NE trending faults and NW trending fractures. We used the daily lake levels in the two reservoirs, from impoundment to 2000, to calculate the time history of the diffused pore pressures and their daily rate of change at the hypocentral locations. The results of our analysis indicate that Episodes I and IV are primarily associated with the initial filling of the two reservoirs. The diffused pore pressures are generated by the large (20-45m) annual fluctuations of lake levels. We interpret that critical excess pore pressures >~300 kPa and >~600 kPa were needed to induce Episodes I to III and Episodes IV to VI respectively, suggesting the presence of stronger faults in the region. The exceedance of the previous water level maxima (stress memory) was found to be the most important, although not determining factor in inducing the episodes. The annual rise of 40 m or more, rapid filling rates and elevated dp/dt values over a filling cycle, contributed to the rapid increase in pore pressure.

Keywords: Reservoir Induced Seismicity, Koyna Reservoir, pore pressure diffusion, stress memory, strain hardening.

1. Introduction

Continuous reservoir induced seismicity (RIS) has been observed since 1963 in the Koyna-Warna region (KWR) after the impoundment of the Koyna Reservoir (in western India) in 1961 and Warna Reservoir in 1985. The seismicity covers a volume ~30 km long, ~20km wide and ~10km deep. Through 2006, more than 100,000 earthquakes have been recorded, including more than 170 events with M ≥4 and 19 events with M ≥5 (henceforth referred as M5 events) with non-repetitive epicenters (Gupta, 2002; Gupta et al., 2007). Over the years, the KWR has been the subject of

numerous studies (see e.g. in the last two decades, Gupta 1992; Talwani et al., 1996; Talwani, 1997b; Rastogi et al., 1997; Mandal et al., 1998; Talwani, 2000; Gupta 2002; Gupta et al., 2002; Gupta et al., 2005; Satyanarayana et al., 2005; Kumar et al., 2006; Gupta et al., 2007; Sarma and Srinagesh, 2007; Chadha et al., 2008). A few studies have been aimed at understanding the mechanism of RIS at the KWR (e.g. Simpson et al., 1988; Kalpna and Chander, 2000; Talwani, 1995, 1997a; Rajendran and Harish, 2000; Pandey and Chadha, 2003).

A unique observation in the region is the continuing occurrence of M5 earthquakes, 44 and 20 years after the impoundment of Koyna and Warna Reservoirs respectively. In this paper, we combine our improved understanding of both the seismotectonic framework of the KWR and mechanism of RIS in order to explain the RIS and hydromechanics of the KWR, by a study of the pore pressure history associated with the spatial and temporal evolution of M5 earthquakes. We chose M5 events because of their non repeating hypocentral locations, each of which was associated with a ~10 km^2 rupture area. Understanding the origin of these earthquakes is challenging and fascinating, and is the subject of this study.

We first present the revised seismotectonic framework of the KWR in light of results of studies of recent seismicity and geophysical investigations. We suggest the association of various fractures and faults with the M5 earthquakes. Our analysis suggests that the saturated fractures in the KWR are critically stressed (Section 2). Next we describe our understanding of the predominant role of pore pressure diffusion (Chen and Talwani, 2001) in isolated, discrete fractures (Cornet and Yin, 1995; Talwani et al, 1999; Evans et al., 2005; Talwani et al., 2007) in the onset of RIS due to lake level fluctuations.

We address (a) the role of long-period lake level fluctuations (Roeloffs, 1988) on the diffusion of pore pressure to large distances; (b) the increase in pore pressures to threshold levels to induce M5 earthquakes; (c) the observation that large dp/dt changes help trigger RIS (Nur and Booker, 1972; Talwani et al., 2007) (Section 3). Then we present observations that show that some of the episodes of M5 earthquakes show evidence of stress memory in this large, critically stressed volume. (Section 4). The specific goals of this study to understand the hydromechanics of the KWR are described in Section 5. To achieve them, we use the daily lake level data at Koyna and Warna Reservoirs up to 2000 and the assumption of one dimensional pore pressure diffusion through fractures comprising the seismotectonic framework to calculate the pore pressure (p) and the rate of pore pressure change (dp/dt) histories at hypocentral locations of M5 earthquakes (Section 6).

We conclude that the continued occurrence of seismicity in the KWR for more than 45 years is a result of a combination of factors, which include (a) the renewed generation of pore pressure (~100s kPa) due to large (20-45m) annual fluctuations of lake levels of Koyna and Warna Reservoirs; (b) the availability of a network of fractures with permeabilities greater or equal than the seismogenic permeability ($k \geq k_s$) to diffuse pore pressure to large distances in a (c) critically stressed volume (30x20x10 km^3) (d) the cumulative effect of annual cycles of lake level changes contributes to increase the pore pressure to threshold levels; (e) the exceedance of lake levels over the previous maxima; (f) large dp/dt amplitudes and filling rates, which appear to contribute to higher pore pressures; (g) elastic-plastic deformation with strain hardening, which possibly

strengthens the fractures, accounts for the observation of stress memory in this critically stressed volume. (Section 7)

2. Seismotectonic framework in the KWR.

In the KWR the seismicity is associated to lake level changes in the two reservoirs. Figure 1a compares the daily histogram of the number of M≥4.0 recorded earthquakes (catalog from Gupta, 2000) with the lake levels in the two reservoirs since their impoundment in 1961 (KR) and 1985 (WR) to 2000. Figure 1b compares the times of occurrence of M5 events with the two lake levels in and their locations are given in Figure 2.

Talwani (1997b) integrated seismological data from 1962 to 1995 with geomorphic, geological and geophysical data to describe the seismotectonic framework of the Koyna-Warna area. In the revised seismotectonic framework (Figure 2), we use additional information based on the analysis of over 600 digitally recorded earthquakes from April 1996 to December 1997 (Srinagesh and Sarma, 2005; Sarma and Srinagesh, 2007) and magnetotelluric surveys in the Koyna area (Sarma et al., 2004; Harinarayana et al., 2007).

The revised seismotectonic framework (Figure 2) consists of a pattern of crisscrossing steeply dipping, NE trending faults, associated with primarily left-lateral strike slip motion; and a system of sub-parallel, NW trending near vertical fractures, associated with primarily normal faulting; in response to a ~N-S oriented stress field (Talwani, 1997b, Gupta et al. 2002; Sarma and Srinagesh, 2007). The former include the Koyna River fault zone (KRFZ), Donachiwada, Patan, and P1 faults, and the latter include linear features L1 to L7 (Figure 2). (We have renamed the lineaments given in

Talwani (1997b) to follow the nomenclature provided by Gupta et al., 2002). The steep NW-SE trending faults divide the area between the Koyna and Warna rivers into distinct blocks, providing conduits for fluid pressure flow to hypocentral depths.

L3 is a major NW-SE lineament that crosses the Koyna-Warna region and extends up to the Warna dam. It was found by Langston (1981) from the inspection of Landsat images. L1 and L2 are based on the analysis of seismicity data by Talwani et al. (1996) and Talwani (1997b). L4 and L5 are based on aeromagnetic data (Talwani et al., 1996 and Peshwa, 1991). The location of Patan fault is based on geomorphological features and 1994 seismicity data (Talwani et al., 1996; and Talwani, 1997b). P1 is exclusively based on the analysis of seismicity data (Talwani et al., 1996; and Talwani, 1997b). L6 and L7 are based on the revised hypocentral locations obtained by Srinagesh and Sarma (2005) and Sarma and Srinagesh (2007). They divided the revised hypocentral locations into three zones, one of which lies along the Donachiwada fault, the other two NW-SE trending zones were labeled SEZ and WSZ. Cross-sections across WSZ and SEZ show that earthquakes lie along four vertical ~parallel NW-SE trending planes, two of which coincide with L4 and L5 described earlier, and the other two we have named L6 and L7 (Figure 2). The locations of the 19 M5 earthquakes in the KWR are shown in Figure 2, and their causative faults are listed in Tables 1a and 1b.

3. Mechanisms of RIS applied to the KWR

Talwani (1997a) determined that the protracted induced seismicity in the Koyna-Warna region is a consequence of the large annual water level fluctuations associated with the monsoon season. The study of the spatiotemporal pattern of seismicity in the KWR for over four decades, and comparison with the anomalously large (25 to 45m)

annual lake-level fluctuations reveals some unique features. The seismicity is primarily associated with, and delayed with respect to, the large annual filling between June and August, with about two-thirds of the annual seismic energy release occurring from September to December, including the continuing occurrence of M 4 and 5 events long after the initial impoundment (Talwani, 1997b, 2000, Talwani et al., 1996). The seismicity is induced by excess pore pressures associated with the filling, as they diffuse through saturated, critically stressed saturated fractures (Talwani, 1997b; Talwani et al., 2007). It is confined to a ~30km long, 20km wide and 10km deep seismogenic volume (Figure 2).

Several other factors are known to be associated with reservoir induced seismicity (RIS). These include the total height of the water column, the filling rate, the duration of the highest lake level and the amplitude and frequency of the lake level fluctuations (see e.g. Gupta, 2002). Another observation, the occurrence of large magnitude events when the lake level exceeds the previous maximum lake level (Gupta and Combs, 1976; Simpson and Negmatullaev, 1981) was recognized to occur in the KWR for three M 5 events, and the phenomenon, stress memory, to be a crustal manifestation of the Kaiser effect observed in the laboratory (Simpson et al., 1988; Talwani et al., 1996; Talwani, 1996, 2000). More recent studies show that most of the M5 events in the KWR manifest evidence of stress memory (next section).

Assuming a simple 2-D reservoir, Roeloffs (1988) calculated that the stress and pore pressure fields produced by time oscillatory reservoir loading are governed by a dimensionless frequency Ω given by $\Omega = \omega L^2/2c$, where ω is the loading frequency, L is the width of the reservoir and c is the hydraulic diffusivity. The depth below which

diffusion associated with cyclic pore pressure changes at the surface is negligible is given by $z = \pi(2c/\omega)^{1/2}$. Talwani (1997a) calculated this distance for a range of c and ω. For Koyna and Warna Reservoirs (loading frequency is 1/year) he found it to be 25km for $c=1m^2/s$ and 78km for $c=10m^2/s$. Kessels and Kück (1995) showed the applicability of the 1-D diffusion analysis along horizontal fractures. The observation of RIS more than 30 km south of Koyna Reservoir, suggests that the pore pressures associated with the annual filling cycles diffused along fractures connecting the reservoirs to the hypocenters.

Nur and Booker (1972) showed that when aftershocks could be attributed to pore pressure changes, their frequency was proportional to the rate of pore pressure increase. Talwani et al., (2007, Figures 3a and 3b in their paper) showed that the time of occurrence of induced earthquakes at Monticello Reservoir coincided with a peak in the rate of pore pressure change, dp/dt, with time.

In summary, earlier work suggests that RIS is associated with high diffused pore pressures (in accordance with the Coulomb failure criterion) and that is triggered by high dp/dt values. We will test these ideas with over 40 year of lake level and seismicity data from the KWR.

4. Stress Memory

Stress memory of rocks is the ability to accumulate, retain and, under certain conditions, to reproduce information on the stresses experienced in the past (Lavrov, 2003). The Kaiser-effect and strain hardening are manifestations of stress memory in various types of materials (e.g. metals and rocks), and are called stress memory effects (see Lavrov, 2003, for a review). The Kaiser-effect was discovered in the laboratory by Kaiser (1953). During cyclic loading with increasing stress, he observed a marked

increase in acoustic emission activity (or microseismicity) when the largest stress level of the previous cycle was exceeded.

Another possible stress memory effect is strain hardening. Strain hardening is a strengthening mechanism that increases the yield point of a material, i.e. upon reloading a material will not deform plastically further unless the load is increased above its previous level (Hill, 1950; Mendelson, 1983). Strain hardening is associated with plastic contraction of rocks, their subparticles become irreversibly more densely packed, which strengthens their elastic interactions that better withstand the subparticles from being moved apart (Coussy, 1995). Seminal work on elastic-plastic deformation of rocks was carried out by Rice (1975, 1977) and Rudnicki and Rice (1975). Strain hardening can only take place during elastic-plastic deformation of rocks. Given the stress-strain curve of a material, its behavior can be characterized as elastic, elastic-plastic or perfectly plastic, depending on how large the plastic (permanent) strain is with respect to the elastic strain (Mendelson, 1983). In the elastic case, the elastic strain is dominant and the stress-strain curve follows the generalized Hooke's law. In the rigid-plastic or perfectly plastic case, the plastic strain is dominant and the theory of plasticity is applicable. Finally, in the elastic-plastic case, the elastic and plastic strains are comparable, and both the generalized Hooke's law and the theory of plasticity have to be applied. Recent work by Templeton and Rice (2008) and Viesca et al. (2008) examine off-fault elastic-plastic deformation for dry and fluid saturated materials respectively, focusing mainly on the undrained (no fluid diffusion) effects. We suggest from our study that elastic-plastic deformation with strain hardening in drained conditions might explain the phenomena of stress memory observed in the KWR.

4.1. Stress Memory in the KWR

Figure 2 shows the location of the 19 events (M ≥5) plotted on an outline of the revised seismotectonic framework. These 19 events, which include the largest reservoir induced event, M 6.3 in December, 1967, occurred in seven episodes (Tables 1a and 1b). An episode is defined as a sequence of one or more M≥5.0 events that follows the exceedance of a lake level elevation above the previous highest value (Hmax). (Different magnitudes have been listed for the larger events by various workers. In this paper, the magnitudes of these events have been taken from Gupta et al., 2002).

Episode I which includes the M 6.3 main shock in December, 1967, consists of ten M ≥5 events, while the other episodes consist of one or two such events (Tables 1a and 1b). The temporal distribution of these events, vis a vis the water levels in the Koyna and Warna Reservoirs is shown in Figure 1b.

Evidence of stress memory was first realized with the comparison of the daily water level changes with the times of onset of the first three episode of M≥5.0 (Talwani, 1996, 2000; and Talwani et al., 1996). The highest water level and filling rate in any year depends on the annual rainfall between June and August, and on the draw-down governed by engineering considerations. In Figure 3 we show those times when the previous maximum water levels (Hmax) are exceeded (solid dots), and the durations when they are not (horizontal lines). We compare the times of maximum water levels (Hmax) for the Koyna and Warna Reservoirs with the times of Episodes I to VII.

Filling of the Koyna Reservoir started in 1961 and Hmax was exceeded on July 11, 1962, and the new Hmax (636.65m) was reached on August 15, 1962. The initial filling stage lasted until 1965, with an Hmax value of 655.16m. This value of Hmax was

first exceeded on August 30, 1967. It was followed by a M5.2 event (#1) on September 13, 1967. The highest water level observed that year was on October 4, 1967 (656.99m) and the largest reservoir induced event, M6.3, occurred on December 10,1967 (UTC), (4.21 a.m. on December 11,1967 local time). This event was followed by five aftershocks with M≥5.0 in the following two days, and three later, the last one on October 29, 1968 (Gupta et al., 2002).

The farthest event (#8 on December 24, 1967) was located ~20 km to the southeast. Other M ~ 4 aftershocks were located near the present day Warna Reservoir, which had not been impounded at that time (Talwani 1997b). The locations of the aftershocks are probably good to better than ~5km. These ten events constituting the foreshock-main shock- aftershock sequence make up Episode I, and their pattern is similar to RIS at other locations following the initial impoundment (Talwani, 1997a).

The 1967 Hmax (656.99m) was next exceeded on September 2, 1973 and the new Hmax (657.98m) was reached on September 27, 1973. It was followed by a magnitude 5.2 event on October 17, 1973, (earthquake # 11) which constitutes Episode II.

The 1973 Hmax was next exceeded on September1, 1980 and was followed by a M 5.2 event the next day. Hmax (658.13m) was reached on September 3, 1980. It was followed by a M 5.3 event (#13) on September 20, 1980. These two events, which were located more than 25km from Koyna Reservoir constitute Episode III. Earthquake # 13 was associated with the Koyna River fault zone, and earthquake # 12 was located on L5. Talwani (1997b) speculated that these locations were connected to the Koyna Reservoir by a network of crosscutting faults and fractures (Figure 2).

The next episode did not occur until after the impoundment of the Warna Reservoir, which began in 1985. Following its impoundment there were four more episodes of M ≥5 events (Table 1b).

After the initial filling of the Warna Reservoir (1985-1992), the 1992 Hmax (617.90 m) was exceeded on July 3, 1993 and the new Hmax (621.80m) was reached on August 4, 1993. Two M ≥5 events (#14 and #15, constituting Episode IV) occurred on December 8, 1993 and on February 1, 1994 at distances of ~13 and ~25 km from the deepest part of Warna Reservoir (near the dam) respectively, the latter event was associated with normal faulting on the Patan fault. Its aftershocks lie along L2 (Figure 2). These events which occurred 158 and 213 days after the 1992 Hmax was exceeded showed evidence of pore pressure diffusion to the northwest of Warna Reservoir, possibly along the same sets of fractures that were associated with southward pore pressure diffusion from Koyna Reservoir during earlier episodes. We attribute these events to the initial filling of the Warna Reservoir.

The Hmax in Warna Reservoir was next exceeded in September 2, 1994 by 0.25m and then again in 1998 by 3.8m (Table 1b). The next Episode, V, consists of two events that occurred during a period of lake level decline in March and April 2000, about 10km from deeper part of the Warna Reservoir. The March 2000 event occurred after a lag of 562days after the 1994 Hmax was exceeded on August 28, 1998. These two events were the farthest south of the M ≥5 events in the KWR, and occurred in a previously aseismic area.

Earthquake # 18 on September 5, 2000 occurred six days before the 1998 Hmax (625.85m) was exceeded. Although not strictly consistent with our definition of an

episode, we consider earthquake # 18 as a new Episode, VI, because it was associated with a water level rise and the elevation was a few cm of the ultimate Hmax (626.30m). This event was located closer to the reservoir than the previous two.

The 2000 Hmax was exceeded on ~September 10, 2003, and earthquake # 19 constituting Episode VII, occurred on March 03, 2005, 551 days later, during a period of lake level decline.

Summarizing, there have been seven episodes of M ≥5 events in the KWR in the last four decades. The 19 events that make up these episodes did not repeat their hypocentral locations, and are contained in a critically stressed 30x20x10 km^3 volume. Comparing the temporal patterns of these episodes with laboratory data, we can think of Episodes I and IV, which followed the impoundment of the Koyna and Warna Reservoirs, as being associated with the initial filling. We suggest that Episodes II, III, IV, VI and plausibly also V and VII, are manifestation of stress memory on a crustal scale. That is, a ~6,000km^3 seismogenic volume, remembers the water level maximum Hmax that preceded a M ≥5 event, and when that water level is exceeded, even by 0.15m, a new episode occurs.

If the excess lake load, above the previous Hmax was the only contributing factor, it would imply very small triggering stresses associated with these M5 events. Next we examine other possible causes of additional stress perturbations, which are summarized in the next section.

5. Goals of the study

Several factors have been suggested as possible contributors to the development of the critical pore pressure (p_c) and the triggering of M5 events. To obtain an estimate of p_c values associated with various episodes and the relative contributions of different factors, we analyzed the excess pore pressures associated with the filling histories of the two reservoirs. Specifically, we evaluated the contributions of the following factors: (a) the annual cycle of lake level fluctuations; (b) the amplitude of the annual increase in lake level, ΔH, specially for those years when it exceeds 40 m; (c) the maximum rate of pore pressure (dp/dt) increase over a filling cycle, A; (d) exceedance of the lake level over a previous maximum level (identified as a manifestation of stress memory in rocks); (e) the cumulative effect of annual cycles of filling and emptying of the reservoir between episodes; (f) complete leakage or no leakage of built up pore pressures between episode and (g) the combined effect of the two reservoirs.

To study the **relative** contributions of these factors, we calculated the excess pore pressure by assuming simple one-dimensional diffusion of pore pressure through a network of fractures based on our current understanding of the seismotectonic framework. Although the fractures are two-dimensional features, hypocentral locations suggest that only finite strips of the fractures are seismogenic and conduits for pore pressure diffusion. As the details of these are not known, we assumed simple one-dimensional pore pressure diffusion between the reservoirs and the hypocentral locations. The calculated pore pressures may overestimate the true excess pore pressures but they give meaningful estimates of the relative contributions of the various factors.

6. Calculation of diffused pore pressure histories at hypocentral locations

6.1. Theory

Roeloffs (1988) calculated the pore pressure at time t>0 and a depth z due to a change in the level of a reservoir lake behind a dam at time t=0. The total pore pressure at a depth z and time t, p(z,t) can be expressed as the coupled response of diffused pore pressure and undrained pore pressure.

$$p(z,t) = (1-\alpha)\cdot p_0 \cdot erfc\left[\frac{z}{(4ct)^{1/2}}\right] + \alpha \cdot H(t) \cdot p_0 \qquad (1)$$
$$\alpha = B\cdot(1+\nu_u)/\left[3\cdot(1-\nu_u)\right]$$

where erfc is the complementary error function, H(t) is the Heaviside unit step function, B is the Skempton's coefficient, ν_u is the undrained Poisson's ratio, z is the depth beneath the reservoir, p_o is the vertical stress at a depth z=0, c is the hydraulic diffusivity and t is time.

The undrained pore pressure term in equation (1) builds up instantaneously in the vicinity of a reservoir via Skempton effect due to the load of water. For a point load, the undrained pore pressure effect is contained within a cone whose horizontal and vertical dimensions are about 3 to 4, and 6 to 7 times the width of the reservoir (Talwani et al., 2007). For Koyna Reservoir, assuming the deepest part to be adjacent to the dam, and a maximum width of ~2.5km, the undrained pore pressure is contained within a horizontal distance of ~10km and a vertical distance of ~17.5 km. Our study focuses on M5 earthquakes, some of which occurred in the vicinity of Koyna Reservoir within the cone shaped volume with a non-zero undrained effect. We estimate this undrained effect at hypocentral locations within this volume.

The pore pressure increase due to compression (undrained response) at a distance r from the reservoir is

$$\Delta p_u(r) = -B\Delta\sigma_{kk}/3 \tag{2}$$

where $\Delta\sigma_{kk}/3$ is the change in the mean stress at the given distance r. Considering a uniform circular load, Ahlvin and Ulery (1962) tabulated the vertical, radial and transverse stresses at a point at any radial distance from the center of the circular load and at a given depth. Assuming B~0.7 for crystalline rocks (Talwani et al., 1999) and water height of ~70 m, for an earthquake at a depth of 4 km and a radial distance of 2 km, the undrained response is of the order of 20 kPa (Appendix I), one order of magnitude less than the diffused pore pressure values calculated in this study (see next section). Therefore, we disregard the undrained effect in our calculations and consider only the changes in pore pressure due to diffusion. Substituting α=0 (no undrained effect) in equation (1), the diffused pore pressure component can be written as

$$p(z,t) = p_0 \cdot erfc\left[\frac{z}{(4ct)^{1/2}}\right] \tag{3}$$

Rajendran and Talwani (1992) and Chen and Talwani (2001) calculated the diffused pore pressures away from a reservoir. We have revised the formulation following the methodology given in those papers and, applying the principle of superposition to the equation obtained by Roeloffs (1988), the following mathematical expression can be written for one dimensional pore pressure diffusion in any direction:

$$P_n = \delta p_1 \cdot erfc\left[\frac{r}{(4cn\delta t)^{1/2}}\right] + \delta p_2 \cdot erfc\left[\frac{r}{(4c(n-1)\delta t)^{1/2}}\right] + \delta p_3 \cdot erfc\left[\frac{r}{(4c(n-2)\delta t)^{1/2}}\right] + \ldots + \delta p_n \cdot erfc\left[\frac{r}{(4c\delta t)^{1/2}}\right] \tag{4}$$

where δt is a fixed increment of time (i.e. 1 day, see next section), n is the number of time increments considered in our calculation (i.e. number of days), δp_n is the water load change for the nth day, r is the distance from the reservoir, c is the hydraulic diffusivity and erfc is the complementary error function. The equation states that the diffused pore pressure n days after the filling of a reservoir at a distance r from the reservoir is the sum of the diffused pore pressures generated by discrete water load changes in a given time step δt. The first discrete water load change δp_1 contributes for a total of n days to the total diffused pore pressure, while last discrete water load change δp_n contributes only for one day.

We use equation (4) to calculate the diffused pore pressure associated with the impoundment and annual filling cycles of Koyna and Warna Reservoirs at the times and locations of episodes of M5 earthquakes. The water load changes δp correspond to time steps δt of 1 day. The rate of pore pressure change dp/dt is calculated by subtracting the pore pressure values in two continuous days and dividing them by the time step of 1 day. Next we describe how we estimate the distances from the reservoirs to the earthquakes and the hydraulic diffusivity values along the diffusion paths.

6.2. Data and assumptions

Water level data cover the period from 1961 (impoundment) to 2000 for Koyna Reservoir (14,606 data points) and 1985 (impoundment) to 2000 for Warna Reservoir (5,685 data points). Figure 1b shows the daily water level curves for Koyna and Warna Reservoirs, and the times of the episodes (vertical lines). The hypocentral distance from the reservoir, r, assuming that pore pressure diffusion is restricted to faults and fractures (Cornet and Yin, 1995; Talwani et al, 1999; Evans et al., 2005), was estimated from the

inferred paths of pore pressure diffusion along them. The values of hydraulic diffusivity, c, along these paths were obtained from Talwani et al., 2007 (Tables A.1 and A.3 in that paper), and vary between ~1 and 10 m^2/s. Based on this range of values, we calculate diffused pore pressures in the Koyna-Warna region for three values of c, i.e. 1, 5 and 10 m^2/s.

The distance to the hypocenter for pore pressure diffusion, r, was calculated from the dams because they represent the deepest part of the reservoir and water levels are measured next to the dams. In calculating this distance, r, we first estimated the total horizontal distance (x) along the chosen surface path. Then, taking the hypocentral depth (z), we estimated $r=(x^2+z^2)^{1/2}$. Tables 2a to 2c list the estimated values of x, z and r for the different earthquakes. Because of the uncertainties in the estimation of distances, and to obtain meaningful, order of magnitude estimates of the diffused pore pressures, we used a range of representative distances for r, rounded to the nearest 5km (shaded in Tables 2a to 2c).

Given the uncertainties in the horizontal distances along fractures, depths and hydraulic diffusivity values, we calculated the diffused pore pressures for a range of distances and hydraulic diffusivity values. For example, we assigned earthquake # 11 to occur on L1. We assumed the path of pore pressure diffusion from Koyna Reservoir to the hypocenter of earthquake # 11 to be along KRFZ and L1 (Figure 2). Taking the horizontal distances along KRFZ and L1 to be ~2.0 and 4.3 km we get x=6.3km. With the hypocentral depth z=4.0 km, we get the hypocentral distance r=7.5km. We used 5 km and 10 km as representative distances in our calculations of diffused pore pressures. In

common with other earthquakes, the pore pressure for earthquake # 11 was calculated for three values of c, i.e. 1, 5 and 10 m^2/s.

6.3. Pore pressure changes associated with M5 earthquakes

To obtain realistic values of diffused pore pressure we incorporated in our calculations how M5 earthquakes affect the pore pressure field. Muir-Wood and King (1993) found that the character of the hydrological changes that follow major earthquakes depend on the style of faulting. Earthquakes associated with normal faulting expel sizeable amounts of water but earthquakes associated with reverse faulting do not. Their coseismic strain model explains the differences between the hydrological signatures of normal and reverse fault earthquakes. For normal faulting, cracks open and the effective porosity increases during the interseismic period; at the time of an earthquake, cracks close and water is expelled. We interpret that, after the normal faulting earthquake, the pore pressure values are lower that those before the earthquake, there is a leakage (decrease) of pore pressure during normal faulting. For reverse faulting –according to their model-, cracks close and water is expelled during the interseismic period; at the time of an earthquake, cracks open and water is drawn in. We interpret that, after the reverse faulting earthquake, the pore pressure values are higher that those before the earthquake. For strike-slip faulting we have a mixture of the two. Pore pressure values after an earthquake can drop (normal faulting) or increase (reverse faulting) depending on the style of faulting. As normal faulting is the dominant focal mechanism in the Koyna-Warna region (except for the main shock in December, 1967), we expect that there is at least some release of built up pore pressures after each event. In calculating the pore pressure increase following each episode, we considered that a) there is no loss of pore

pressure and that it continuously builds up after impoundment and b) all the built up pore pressure is released (complete leakage) during each episode, and starts to increase afresh in response to the total water column in the reservoir. These two extreme cases comprise any other possibility, where there is a partial release of pore pressures. In the absence of reverse faulting mechanism for any M5 earthquake, we do not consider any pore pressure increase after an episode.

6.4. Observed duration between episodes

From the Coulomb failure criterion assuming no cohesion, a new episode can occur when the pore pressures reach a threshold or critical value (p_c) that depends on the pre-existing stress state and strength of faults,

$$p_c=\sigma_n-\tau/\mu \qquad (5)$$

where σ_n and τ are the normal and shear stresses, and μ is the coefficient of friction. The durations of 5 to 7 years between consecutive episodes (except between V and VI) suggests that there is a partial or complete leakage of pore pressure after each episode, and that this duration reflects the time needed to raise the pore pressure again to seismogenic levels. The following calculation illustrates how the cumulative effect of several years of annual lake level fluctuations can result in a diffused pore pressure increase to critical levels. From Figures 1a and 1b we note that the annual lake level changes in the two reservoirs vary from 20 to 45m. These fluctuations occur above a 'base' water level of about 20-30m in the two reservoirs. So the contributions of the water levels in the reservoirs can be divided into two parts. The first is the contribution of a constant head of water (20-30m) above the pre-impoundment level, and the second due to the annual lake level fluctuations above that level. The contribution of a constant head of

water above pre-impoundment levels can be calculated using equation (4). For $c=1m^2/s$ and at a 5 km distance, the diffused pore pressures reach ~80% of the load six years after impoundment (Figure 4a). For ~20-30m of water, corresponding to a load of 0.2 to 0.3 MPa at the surface, the pore pressure increase is 0.16 to 0.22 MPa after six years. Using equation (4) we evaluate pore pressure changes due to diffusion associated with six annual filling-emptying cycles, at a distance of 5km from a reservoir, assuming $c=1m^2/s$. We note that the maxima in pore pressures lag behind the annual maxima in lake levels, and that the pore pressures increase from about 35% of the load after the first year, to ~55% after 6 years (Figure 4b). For an annual fluctuation of Koyna Reservoir between ~30 to 40m, excluding the small stress release associated with M4 and smaller events, the excess pore pressure at 5km from the reservoir by diffusion alone, would be ~ 0.17 to 0.22 MPa after six years. In summary, the two contributions to the pores pressures at hypocentral depths are of the same order (~0.15 to 0.2 MPa). Both effects need to be taken into consideration when attempting to calculate diffused pore pressures generated after each episode.

6.5. Combined effects of the two reservoirs

Annual seismicity maps of the KWR (Talwani et al., 1996; Talwani, 1997b) show a migration of seismic activity from Koyna Reservoir towards the Warna river region from 1967 to 1983 and then a decrease of activity near Warna River in 1984. This observation suggests that pore pressures generated by Koyna from 1967 to 1983 caused earthquakes along the weakest faults of the Warna region. Pore pressures from Koyna were not sufficient to destabilize the stronger faults (as per the Coulomb failure criterion) and seismicity decreased dramatically. After the impoundment of Warna Reservoir,

diffused pore pressures began to increase again in the region, adding up to the pore pressures generated by Koyna. The sudden increase of seismicity in 1993 suggests that the combined diffused pore pressure (from Koyna and Warna) was able to destabilize stronger faults in the KWR. Episode IV consists of earthquakes # 14 and # 15 which occurred in December 1993 and February 1994 (Table 1a and 1b). While earthquake # 14 occurred near Warna Reservoir, earthquake # 15 occurred near Koyna Reservoir (Figure 2). Interestingly, earthquake # 15 was the first M5 earthquake to occur near Koyna after 1973 (Episode II). This observation suggests that it required the combined effect of Koyna and Warna Reservoirs to cause the occurrence of earthquake # 15. If we consider the Patan fault, where earthquake # 15 occurred, is stronger than the surrounding faults near Koyna, we can understand why pore pressures from Koyna alone were unable to destabilize the fault. In 1994, nine years after the impoundment of Warna, the combined effect of both reservoirs provided adequate pore pressure to destabilize the fault and generate earthquake # 15. Possible explanations for the inference of a stronger fault include differences in the rheological properties and the orientation of the fault with respect to the regional stress field. We also suggest that the presence of fluids and changing pore pressures could have facilitated elastic-plastic deformation with strain hardening in the fault. In such case, the strain hardening provided a strengthening mechanism for rocks in the KWR, which would explain the need for increased time and increased pore pressures to destabilize the causative faults.

6.6. Results

We calculate the pore pressure and dp/dt histories for different distances from the assumed time of start of pore pressure accumulation (t_0) to the time of the episode (t_E).

We present two curves for episodes occurring after the initial impoundment, Episode I for Koyna Reservoir and Episode IV for Warna Reservoir. The first curve assumes no leakage of pore pressure after an episode, while the second one assumes complete leakage. For the former, t_0 is the start of impoundment in January 1961 for Koyna Reservoir and June 1985 for Warna Reservoir. For the latter, pore pressures are calculated at the end of the previous episode (I, II, IV and V). For each case, we present the corresponding lake level data between t_0 and t_E, as well as the pore pressure and dp/dt histories at various distances for the different values of the hydraulic diffusivity c. The representative distances, r, for each episode are given in Tables 2a to 2c.

In Tables 3a to 3c, we present the calculated pore pressure at time t_E at the chosen distances for three values of c (1, 5 and 10 m^2/s). For example, the pore pressure due to diffusion for an assumed $c=1m^2/s$ at distances of 5 and 10 km for Episode I (December, 1967) are 450 and 320 kPa (Figure 5 and Table 3a).

For episodes after the impoundment of Warna Reservoir, we add the pore pressure due to diffusion at the hypocentral distances due to both Koyna and Warna Reservoirs. Next we present our selected values of r and c for each episode and the calculated pore pressures due to diffusion.

6.6.1. Excess pore pressures associated with episodes of M5 earthquakes in the KWR

Episode I, consisting of 10 earthquakes, took place during 1967 and 1968 (Tables 1a and 1b). As the depth of the foreshock (event # 1) is not known, we calculate the pore pressure corresponding to the location and time of the M6.3 main shock on December 1967 (# 2). To account for any uncertainties in the hypocentral distance r (estimated at

~10 km, Table 2a) and hydraulic diffusivity c (estimated at 1.7 m^2/s; Talwani, 1981; Talwani et al., 2007), we calculate the diffused pore pressure at distances of 5 and 10 km, and for hydraulic diffusivities of 1 and 5 m^2/s (Table 3a, Figures 5 and 6). Note that Figure 6 covers the period from initial impoundment to the time of Episode I. The largest value of pore pressure, 560 kPa, corresponds to r= 5km and c= $5m^2/s$, whereas the smallest value, 320kPa, corresponds to r=10 km and c=1 m^2/s (Table 3a). We treat this range, 320 to 560 kPa, as a plausible range of excess pore pressure required to induce Episode I.

For subsequent episodes, we consider two scenarios. In the first, there is no leakage of built-up pore pressure after an episode; in the second, there is complete leakage after an episode and the build up pore pressure starts afresh.

For Episode II, the selected hypocentral distances are 5 and 10 km, while the hydraulic diffusivity is 5 m^2/s in view of the increased hydraulic diffusivities (Talwani, 1981; Talwani et al., 2007) immediately after the 1967 main shock, and ~$1m^2/s$ (Talwani, 1981; Talwani et al., 2007) immediately preceding the 1973 earthquake (Episode II). For hypocentral distances of 5 and 10 km, assuming c=5 m^2/s and no leakage of pore pressure, we obtain diffused pore pressures of 540 and 430 kPa (Table 3a, Figure 7, vertical yellow line). In the case of complete leakage of pore pressure after Episode I (Figure 8), the time for start of building up of pore pressure is immediately after Episode I, and the duration of pore pressure increase is from 1968 to 1973. For the same range of values of r and c, the corresponding pore pressures are 530 and 400 kPa. Thus we find the plausible range of excess pore pressure between 400 kPa (with complete leakage of pore

pressure after Episode I, and a hypocentral distance of 10km) and 540 kPa (for no leakage and a hypocentral distance of 5 km).

Episode III occurred seven years after Episode II, 30 km away from Koyna Reservoir (Table 2a). Estimates of the hydraulic diffusivity in the region suggest values of c between 5 and 10 m^2/s (Rastogi et al., 1997; Talwani et al., 2007). For this range of c and a 30 km hypocentral distance, we obtain pore pressures values ranging from 380 to 420 kPa for the case of no leakage, and 290 to 360 kPa for the case of complete leakage (Table 3a, Figures 7 and 9). Thus for Episode III, the plausible range of excess pore pressure by diffusion ranges between 290 kPa and 420 kPa.

For Episode IV, V and VI, we add the combined build up of pore pressure at hypocentral locations due to the water level fluctuations in both reservoirs. Estimates of the hydraulic diffusivity from July to August 1993 in the area close to Warna Reservoir (Rastogi et al., 1997) suggest c=6.9 m^2/s. Correspondingly, we selected two values of c to estimate pore pressures, 5 and 10 m^2/s. Figures 10 and 11 show the diffused pore pressure histories at 10, 15 and 20 km for c=5 and 10 m^2/s assuming no leakage. The first part of Figures 10 and 11 has been replotted for r=15 km -corresponding to earthquake # 14 in Episode IV- and different values of c (Figure 12).

Earthquake # 14 (Episode IV) occurred ~15km away from Warna (Table 2c) and ~30km away from Koyna (Table 2b). Pore pressure values due to Koyna at the hypocentral location range from 360 kPa (with complete leakage of pore pressure during Episode III and c=5m^2/s; Table 3b) to 460 kPa (for no leakage of pore pressure and c=10m^2/s; Table 3b). Pore pressure values due to Warna Reservoir at the hypocentral location range from 290 kPa (for c=5m^2/s; Table 3c; Figures 12) to 350 kPa (for

c=10m^2/s; Table 3c; Figure 11). Therefore, adding the effects of the two reservoirs, the plausible excess pore pressure values could vary between 650 kPa and 810 kPa.

Earthquake # 15 (Episode IV) took place ~15 km away from Koyna Reservoir (Table 2b) and ~30 km away from Warna Reservoir (Table 2c). Pore pressure values generated by Koyna Reservoir at these distances and time of the earthquake vary from 480 kPa (with complete leakage of pore pressure during Episode III and c=5m^2/s; Table 3b) and 540 kPa (for no leakage of pore pressure and c=10m^2/s; Table 3b). For this earthquake, pore pressure values due to Warna Reservoir range from 180 kPa (for c=5m^2/s; Table 3c) to 240 kPa (for c=10m^2/s; Table 3c; Figure 11). The combined effect of both reservoirs generated the earthquake, with plausible excess pore pressures ranging from 660 kPa to 780 kPa.

Episode V (earthquakes # 16 and # 17) occurred ~30 km away from Koyna Reservoir (Table 2b) and ~20 km away from Warna Reservoir (Table 2c). The range of pore pressures generated by Koyna Reservoir at the hypocentral location and time of the earthquake range from 290 kPa (with complete leakage of pore pressure during Episode IV and c=5m^2/s; Table 3b) and 490 kPa (for no leakage of pore pressure and c=10m^2/s; Table 3b). Similarly, the range of pore pressures due to Warna Reservoir varies from 330 kPa (with complete leakage of pore pressure during Episode IV and c=5m^2/s; Table 3c; Figure 13) to 420 kPa (for no leakage of pore pressure and c=10m^2/s; Table 3c; Figure 11). Therefore, after combining the effect of the two reservoirs, plausible excess pore pressure values range from 620 kPa and 910 kPa.

Episode VI (earthquake # 18) occurred after the monsoon rains, five months after Episode V, at 15km distance from Warna Reservoir (Table 2c) and 30 km distance from

Koyna Reservoir (Table 2b). The two previous earthquakes in March and April of 2000 were associated with normal faulting and, therefore, we should expect to have leakage of pore pressure in the hypocentral area associated with Episode VI. The range of pore pressures generated by Koyna Reservoir at the hypocentral location and time of the earthquake range from 4kPa (with complete leakage of pore pressure during Episode V and $c=5m^2/s$; Table 3b) to 490 kPa (for no leakage of pore pressure and $c=10m^2/s$; Table 3b). Similarly, the range of pore pressures due to Warna Reservoir varies from 70 kPa to 400 kPa (Table 3c). The combined excess pore pressures range from 74kPa to 890kPa. This large range is not consistent with those obtained for the previous episodes, the reason being the short period to build up pore pressures after Episode V. Bearing in mind that the interval of time required to build up pore pressures from episode to episode has been normally 5 to 7 years, we do not fully understand how Episode VI followed Episode V in such brief amount of time. Pore pressures might have not dropped as expected during the two previous normal faulting earthquakes (Episode V) in the absence of fractures extending up to the surface (Muir-Wood and King, 1993). This is the subject of future research.

6.6.2. Excess pore pressure associated with M~4.0 earthquakes in the KWR

For comparison, we calculate the required diffused pore pressure to generate a M4 earthquake in the Warna and Koyna areas.

Given the scarcity of seismic stations near Koyna in the early years of seismicity (before 1967), earthquakes were poorly located and any attempt to calculate the diffused pore pressures is subject to the error associated with the earthquake location. The first reported M3.8 earthquake near Koyna Reservoir occurred in 1965/11/06 (lat. 17.4202°,

long. 73.7623°) (Talwani et al., 1996) at a depth of 5 km. Considering the horizontal distance along the main fractures to be ~2.6 km, we obtain a hypocentral distance r of ~6 km from the Koyna dam. Assuming the hydraulic diffusivity to be c=0.1 m^2/s (Talwani et al., 2007) and using equation (4), pore pressures of the order of ~160 kPa are needed to generate a M3.8 earthquake near Koyna.

The first M4.0 earthquake generated after the impoundment of Warna Reservoir occurred on January 6, 1991 near Warna Reservoir at a depth of 6.3 km (lat. 17.1973°, long. 73.7355°) (Talwani et al., 1996). Following the argument given earlier, both Koyna and Warna Reservoir contributed to the diffused pore pressure values and their combined effect caused the earthquake. From the Warna dam, the hypocentral distance is ~18 km (the horizontal distance along the main fractures is ~17 km, considering that pore pressure flows through the lake, L4, P1 and L5). For a hydraulic diffusivity c=5 m^2/s (Rastogi et al., 1997 obtained c=6.9 m^2/s near Warna from July to August 1993, time at which the seismicity near Warna increased dramatically), applying equation (4) we obtain that Warna contributed with diffused pore pressures of the order of ~180 kPa. From Koyna dam, the hypocentral distance is about 26 km (assuming that pore pressures flow through KRFZ and L5). For c=5m^2/s, the pore pressure values from Koyna varies from 340 kPa (assuming complete leakage of pore pressure after Episode III) to 420 kPa (without leakage). Therefore, for c=5 m^2/s, the first M4 earthquake associated with the combined effect of Koyna and Warna Reservoirs occurred at diffused pore pressure values of 520 kPa to 600 kPa.

6.6.3. Amplitude of the annual dp/dt increase

We compare the excess pore pressure (in 10^5 Pa or 100s of kPa –middle panel) with its daily rate of change (dp/dt, in 10^3 Pa/day or kPa/day –bottom panel) at Koyna (1961-1990) and Warna Reservoirs (1985-2001) for two diffusivity values each, in Figures 5, 7, 10 and 11 respectively. Note that the calculated excess pore pressure values reflect the cumulative effect of water level fluctuations from t_0 to a given time t. The calculated dp/dt values reflect the changes in those cumulative pore pressures, and are not directly related to the lake level changes in that cycle. We estimated the amplitude of the annual dp/dt increase, A (Figure 7). It is those changes in dp/dt for a given cycle that we compare with values of ΔH(m) and excess diffused pore pressures.

6.6.4. Comparison of the roles of various factors influencing RIS

Next, for various filling cycles, we compare those factors that have been related to RIS in Tables 4a and 4b. In deciding the filling cycles for comparison, we chose those that included the occurrence of an episode, or in which the lake level exceeded the previous maximum, i.e. displayed stress memory; or the amplitude of the annual increase in water level (ΔH) exceeded 40 m. As we are interested in the relative values of A, for various filling cycles, we calculated it assuming $c=5m^2/s$ at a 10 km distance.

For those filling cycles associated with an episode, the excess pore pressures were calculated at the hypocentral locations and times of the given episodes as described in Section 6.6.1.

For those filling cycles associated with large ΔH and A, but not accompanied by an episode, we calculated the excess pore pressure at the hypocentral location of the next known episode on December 31 of the given filling cycle (middle of the cycle). For all

those filling cycles after Episode II, we calculated these pore pressures assuming both complete leakage of pore pressure following an episode and $c=5m^2/s$ and no leakage with $c=10m^2/s$. The calculated values of the excess pore pressure define the range of possible values for that particular case. We account for the effect of both reservoirs for filling cycles after 1985.

We summarize our findings in Table 4a. For a given filling cycle (column 2), if the maximum water level exceeds the previous maximum water level from Tables 1a and 1b (column 3) and an episode follows, we consider it as evidence of stress memory (we highlight and label and the corresponding cell as 'yes'). If the annual lake level increase (ΔH, column 4) exceeds 40m, we consider it anomalous and highlight the corresponding cell. If the amplitude of the annual dp/dt increase, A (column 5) is more than 1.80 kPa/day, we consider it anomalous and highlight the corresponding cell. We note the occurrence of an episode (column 6), the estimated minimum excess pore pressure, with complete leakage (column 7) and maximum pore pressure with no leakage (column 8). Next we compare these set of parameters for the various filling cycles.

From Section 6.6.1 and Table 4a we notice that after the first episode which was associated with initial filling, Episodes II and III occurred when p_c was greater than ~300 kPa, whereas the subsequent episodes occurred when p_c exceeded ~600 kPa.

For Episode I the values of ΔH(m) and A(kPa/day) were not anomalous, but the previous water level was exceeded. The pore pressure increased to ~560 kPa and induced a M6.3 earthquake and its aftershocks. This behavior of the lake level and seismicity is characteristic of RIS associated with initial filling (Talwani, 1997a). For Episode II, we note that the previous Hmax was exceeded, ΔH and A were anomalously high, and the

minimum induced pore pressure (assuming leakage) was ~400 kPa. In 1975, although ΔH and A were anomalously high, the minimum excess pore pressure ~130 kPa was less than the values obtained for Episodes I, II and III. Only after the 1979-1980 filling cycle, the excess pore pressures at 30 km distance increased enough to cause Episode III. However, Episode III did not occur until the 1980-1981 filling cycle when the lake level exceeded the previous maximum. For the 1992-1993 filling cycle, ΔH and A were anomalously large at Koyna and large excess pore pressures were reached without inducing an episode. Episode IV occurred the following year when Hmax was exceeded at Warna and ΔH and A were anomalously high. For the 1995-1996 and the 1996-1997 filling cycles, ΔH was anomalously high and the minimum excess pore pressures were less than 500 kPa and there were no episodes. For the 1998-1999 filling cycle, there was evidence of exceedance of Hmax, large A and ΔH at Warna, and the minimum excess pore pressure was ~540 kPa and no earthquake occurred, suggesting that p_c had not been reached. Episode V occurred during the 1999-2000 filling cycle which did not show any evidence of stress memory or anomalously high values for ΔH and A, but for which the excess minimum pore pressure exceeded ~600 kPa. For the 2000-2001 filling cycle, the lake level at Warna exceeded the previous maximum and there were no anomalous changes in ΔH or A, and the minimum excess pore pressure exceeded ~74 kPa and episode VI followed. This low value of the minimum excess pore pressure suggests that the excess pore pressure may not have completely leaked following Episode V. The exact cause of this earthquake is not understood.

In order to evaluate the role of filling rate, dH/dt, and the duration of the highest lake level in a filling cycle, D in days, in inducing RIS (see e.g. Gupta, 2002), we

examined these parameters for the filling cycles examined in Table 4a. In some years the lake level begins to rise following the onset of the monsoon in June, and rises to a maximum level and then decreases; we used the dates and heights of the lowest and the highest water levels to calculate the filling rate, dH/dt. In other years, the lake level rises following the initial rains, and then decreases and then goes up again to the highest level in that filling cycle; this usually happens following delayed rains in September. We used the water level attained after the initial filling to calculate dH/dt, and compare it with other years (Table 4b).We counted the number of days, D, that the water level stayed above elevations of 651m and 615m (arbitrarily decided) for the Koyna and Warna reservoirs. These levels are within 10m of the maximum levels attained by the reservoirs. As we were interested in the relative roles of these factors for the different filling cycles, we arbitrarily chose >0.75m/d for the filling rate, dH/dt, and >160days for D, to define as "high" (Table 4b).

In Table 4b, using data for the two reservoirs, we note that four of the six episodes occurred when the filling rates were high, and that there were four instances of these high filling rates without an episode. Of the seven cycles when D was high, only three were accompanied by an episode. These observations suggest that high filling rates and longer duration of high water levels are not the primary factors in inducing an episode, but play a supporting role, if the diffused pore pressures have nearly reached threshold levels.

Next we summarize these observations of the comparative role stress memory and anomalous values of ΔH, A, dH/dt and D in the triggering of episodes (Table 5), and discus them in next section.

7. Discussion and conclusions

In this paper we have attempted to examine the hydromechanics related to the occurrence of six of the seven episodes of reservoir induced M5 events from 1967 to 2005 in the Koyna-Warna region. The seismicity is related to the increase in pore pressures to threshold levels, with the subsequent slippage along the fractures and fault planes identified in the seismotectonic framework. The increase in pore pressure at hypocentral locations large enough to induce the episodes results from changes in surface loads due to lake level fluctuations. We assumed 1-D pore pressure diffusion from the reservoirs to hypocentral locations through a network of fractures. Using the daily lake level data, from the time of impoundment up to 2000, we calculated a history of diffused pore pressure, p, and dp/dt at hypocentral locations. For our calculations, we used a range of values of the hypocentral distance, r, and the hydraulic diffusivity of the involved fractures, c, so as to bracket the true conditions. To account for the release of accumulated pore pressures at the time of M5 events, we calculated the pore pressure increase for the subsequent events by assuming both a complete leakage of pore pressure and a complete absence of leakage at the time to the preceding event, thus further bracketing the real situation.

The episodes occur when the excess pore pressures at the hypocentral locations attained a critical value, p_c, in accordance with the Coulomb failure criterion. In the Koyna-Warna region, the annual cycle of reservoir's filling and emptying contributed to the diffusion of fluid pressures to tens of km. The amplitude of lake level fluctuations, ΔH, and the pre-fluctuation lake levels control these excess pore pressures. For Episodes II and III, the critical excess pore pressures were found to be ~300 kPa or more, whereas

for the subsequent episodes they were ~600 kPa or more. The need for higher pore pressures to induce Episodes IV, V and possibly VI could be because of rheological differences or unfavorable orientation of the fault planes with respect to the regional stress field.

Most of these episodes were associated with normal faulting, which suggested leakage of the excess pore pressures following these events. This assumption was found to be consistent with the observation that 5 to 7 years elapsed between episodes. Our calculations further support this assumption, that 5 to 7 years are needed to build up the excess pore pressures to critical levels.

The role of five factors was examined in the triggering of these episodes after the excess pore pressures had reached critical levels (Table 5). We note that water level exceeded the previous maximum for five of the six episodes. For two cases where the previous Hmax was exceeded, no episode followed in that cycle. Additionally, for the 2003-2004 filling cycle in Warna, the lake level also exceeded the previous Hmax and the M5 event did not occur until the following filling cycle (Table 1b). This observation suggests that in these cases the excess pore pressure had not reached critical values. We conclude that the exceedance of ΔH (stress memory) plays an important but not decisive role in the triggering of these episodes.

For the cases in which ΔH exceeded 40 m and A exceeded 1.80 kPa/day, only two were associated with episodes. There were seven cases when ΔH exceeded 40 m and five cases when A exceeded 1.80 kPa/day and no episode occurred. This suggest that large values of ΔH and A contribute towards the general increase of excess pore pressures but do not induce the episodes. Also for four episodes the filling rate was >0.75m/d, and

there were four occasions where these high filling rates were not accompanied by an episode. Anomalous durations, D, were found to occur before three episodes, while on four occasions there were no episodes. Faster filling rates (see e.g. Figure 5 in Talwani et al., 2007) and longer durations of D contribute to higher diffused pore pressures and at earlier times. We estimate that these two factors contribute a few additional kPa of pore pressure in the diffusion process. They are inadequate of themselves to induce the episodes.

The words 'induced' and 'triggered' have been used interchangeably to describe the seismicity that follows reservoir impoundment or lake level fluctuations. Our results at KWR allow us distinguish between them. We suggest that the seismicity results from a two-step process. The impoundment of a reservoir (in the case of initial seismicity), or large annual lake level fluctuations (in the case of protracted seismicity) over a prolonged period of time, raises the pore pressure by ~100s kPa, which induces the seismicity. Short-term factors (such as the exceedance of the lake level over the previous maxima, large values of H, ΔH. dH/dt, D, dp/dt and A), with pore pressure changes of 10s kPa or less, are the end products of the induction process - advancing the timing of the earthquakes and triggering them.

We did not have daily lake levels after 2000 to analyze Episode VII in 2005. However, based on the limited data, we note that the Hmax was exceeded in Warna reservoir in the third filling cycle (September 2003) after Episode VI. These three cycles were inadequate to generate excess pore pressures to induce any event. It was in the next filling cycle that Episode VII occurred in 2005, 4.5 years after episode VI. Episode VII

was preceded by high filling rates in both the reservoirs (Gupta et al., 2005 and Satyanarayana et al. 2005).

We expect that the seismicity will expand to the southwest of Warna Reservoir, where another M5 earthquake might occur in the future, and whose timing may be advanced if the current Hmax is exceeded.

8. Acknowledgements

This paper benefited from critical comments by David Simpson, Hari Rajaram and an anonymous reviewer. We appreciate the invitation of the Editor Cezar Trifu to submit this paper, and his patience and input in its publication.

9. References.

Ahlvin, R.G., and Ulery, H.H. (1962), Tabulated values for determining the complete pattern of stresses, strains, and deflections beneath a uniform circular load on a homogeneous half space, Highw. Res. Board, Bull. 342, 1–13.

Chadha, R.K., Kuempel, H.-J., and Shekar, M. (2008), Reservoir Triggered Seismicity (RTS) and well water level response in the Koyna-Warna region, India, Tectonophysics, 456, 94-102.

Chen, L., and Talwani, P. (2001), Mechanism of initial seismicity following impoundment at the Monticello Reservoir, South Carolina, Bull. Seism. Soc. Am., 91, 1582-1594.

Cornet, F.H., and Yin, J. (1995), Analysis of induced seismicity for stress field determination and pore pressure mapping, Pure Appl. Geophys., 145, 677–700.

Coussy, O., Mechanics of Porous Continua (John Wiley & Sons, 1995) 472pp.

Dziewonski, A.M., Ekstro, M.G., Franzen, J.E., and Woodhouse, J.H. (1988), Global Seismicity of 1980: Centroid-Moment Tensor Solutions for 515 Earthquakes, Phys. Earth and Planet. Inter. 50, 127–154.

Evans, K.F., A. Genter, and J. Sausse (2005), Permeability creation and damage due to massive fluid injections into granite at 3.5 km at Soultz: 1. Borehole observations, J. Geophys. Res., B04203, doi:10.1029/2004JB003168.

Gupta, H.K., Reservoir Induced Earthquakes, (Elsevier Publishers, Amsterdam 1992).

Gupta, H.K. (2002), A review of recent studies of triggered earthquakes by artificial water reservoirs with special emphasis on earthquakes in Koyna, India, Earth-Science Rev., 58, 279-310.

Gupta, H.K., and Combs, J. (1976), Continued seismic activity at the Koyna Reservoir site, India, Eng. Geol., 10, 307-313.

Gupta, H.K., Ram Krishna Rao, C.V., Rastogi, B.K., and Batia, S.C. (1980), An Investigation of Earthquakes in Koyna Region, Maharashtra, for the Period October 1973 Through December 1976, Bull. Seism. Soc. Am., 70, 1833–1847.

Gupta, H.K., Mandal, P. and Rastogi, B.K. (2002), How long will triggered earthquakes at Koyna, India continue?, Curr. Sci. 82, 202-210.

Gupta, H.K., Mandal, P., Satyanarayana, H.V.S., Shashidhar, D., Sairam, B., Shekar, M., Singh, A., Devi, E.U., Kousalya, M., Rao, N.P., Dimri, V.P. (2005), An earthquake of M~5 may occur at Koyna, Curr. Sci. 89, 747-748.

Gupta, H., Shashidhar, D., Pereira, M., Mandal, P., Rao, N.P., Kousalya, M. Satyanarayana, H.V.S. and Dimri, V.P. (2007), Earthquake forecast appears feasible at Koyna, India, Current Science, 93, 843-848.

Harinarayana, T., Patro, B.P.K., Veeraswamy, K., Manoj, C., Naganjaneyulu, K., Murthy, D.N., and Virupakshi, G. (2007), Regional geoelectric structure beneath Deccan Volcanic Province of the Indian subcontinent using magnetotellurics, Tectonophysics, 445, 66-80.

Hill, R., The mathematical theory of plasticity (Oxford, Clarendon Press, 1950).

Kaiser, J. (1953), Erkenntnisse und Folgerungen ays der Messung von Gerauschen bei Zugbeanpruchung von metalliscen Werstoffen, Archiv fur das Eisenhuttenwesen, 24, 43-45. (in German).

Kalpna and Chander, R. (2000), Green's function based stress diffusion solutions in the porous elastic half space for time varying finite reservoir loads, Phys. Earth Planet. Inter., 120, 93-101.

Kessels, W. and J. Kück (1995), Hydraulic Communication in Crystalline Rock Between the Two Boreholes of the Continental Deep Drilling Project in Germany, Int. J. Rock Mech. Min. Sci. & Geomech. Abstr., 32, 37-47.

Kumar, B. A., Ramana, D.V., Kumar, Ch.P., Rani, V.S., Shekar, M., Srinagesh, D. and Chadha, R.K. (2006), Estimation of source parameters for 14 March 2005 earthquake of Koyna-Warna region, Current Science, 91, 526-529.

Langston, C. A. (1981), Source Inversion of Seismic Wave Form : The Koyna India Earthquake of 13, September 1967, Bull. Seism. Soc. Am., 71, 1–24.

Langston, C. A., and Franco-Spera, M. (1985), Modeling of the Koyna, India, Aftershock of 12 December 1967, Bull. Seismol. Soc. Am. 75, 651–660.

Lavarov, A. (2003), The Kaiser effect in rocks; principles and stress estimation techniques, Intl. J. Rock Mech. Mining Sciences, 40, 151-171.

Mandal, P., Rastogi, B.K. and Sarma, C.S.P. (1998), Source parameters of Koyna earthquakes, India, Bull. Seism. Soc. Am., 88, 833-842.

Mendelson, A., Plasticity: Theory and Application (Krieger, 1983).

Muir-Wood, R., and King, G.C.P. (1993), Hydrological signatures of earthquake strain, J. Geophys. Res., 98, 22,035-22,068.

Nur, A., and J. R. Booker (1972), Aftershocks caused by pore fluid flow?, Science, 175, 885– 887.

Pandey, A.P. and Chadha, R.K. (2003), Surface loading and triggered earthquakes in the Koyna-Warna region, western India, Phys. Earth Planet. Inter., 139, 207-223.

Peshwa, V. V. (1991), Geological Studies of Chandoli Dam Site Area Warna Valley, Sangli Dist., Maharashtra State. Studies Based on Remote Sensing Techniques. Unpublished Report to Maharashtra Engineering Research Institute, Nashik, Department of Geology, University of Pune, 45 pp.

Rajendran, K. and Talwani, P. (1992), The role of elastic, undrained, and drained responses in triggering earthquakes at Monticello Reservoir, South Carolina, Bull. Seism. Soc. Am., 82, 1867-1888.

Rajendran, K. and Harish, C.M., (2000), Mechanism of triggered seismicity at Koyna: an assessment based on relocated earthquake during 1983– 1993, Curr. Sci., 79, 358–363.

Rao, B.S.R., Prakasa Rao, T.K.S., and Rao, V.S. (1975), Focal Mechanism Study of an Aftershock in the Koyna Region of Maharashtra State, India, Pure Appl. Geophys. 113, 483–488.

Rastogi, B.K., Chadha, R.K., Sarma, C.S.P., Mandal, P., Satyanarayana, H.V.S., Raju, I.P., Kumar, N., Satyamurthy, C. and Rao, A.N. (1997), Seismicity at Warna Reservoir (near Koyna) through 1995, Bull. Seism. Soc. Am., 87, 1484– 1494.

Rice, J.R. (1975), On the stability of dilatant hardening for saturated rock masses, J. Geophys. Res., 80, 1531-1536.

Rice, J.R. (1977), Pore pressure effects on inelastic constitutive formulations for fissured rock masses, Advances in Civil Engineering Through Engineering Mechanics, Proceeding of 2nd ASCE Engineering Mechanics Division Specialty Conference, N.C. Raleigh, 1977, pp. 295-297, Am. Soc. of Civ. Eng., New York.

Roeloffs, E.A. (1988), Fault stability changes induced beneath a reservoir with cyclic variations in water level, J. Geophys. Res., 83, 2107– 2124.

Rudnicki, J.W. and Rice, J.R. (1975), Conditions for localization of deformation in pressure-sensitive dilatant materials, J. Mech. Phys. Solids, 23, 371-394.

Sarma, S.V.S., Prasanta, B., Patro, K., Harinarayana, T., Veeraswamy, K., Sastry, R.S., and Sarma, M.V.C. (2004), A magnetotelluric (MT) study across the Koyna seismic zone, western India: evidence for block structure, Phys. Earth and Planet Interiors, 142, 23-36.

Sarma, P.R., Srinagesh, D. (2007), Improved earthquake locations in the Koyna-Warna seismic zone, Nat. Hazards, 40, 563-571.

Satyanarayana, H.V.S., Shashidhar, D., Sagara Rao, T. and Kousalya, M. (2005), An *M* 5.2 earthquake occurs in Koyna region after 4 1/2 years, Curr. Sci. 89, 612-613.

Simpson, D.W. and Negmatullaev, S.K. (1981), Induced seismicity at Nurek Reservoir, Tadjikistan, USSR. Bull. Seism. Soc. Am., 71, 1561–86.

Simpson, D.W., Leith, W.S. and Scholz, C.H. (1988), Two types of reservoir-induced seismicity, Bull. Seism. Soc. Am., 78, 2025-2040.

Srinagesh, D., and Sarma, P.R. (2005), High precision earthquake locations in Koyna-Warna seismic zone reveal depth variations in brittle-ductile transition zone, Geophys. Res. Lett., 32, 8310-8313.

Talwani, P. (1981), Hydraulic diffusivity and reservoir induced seismicity, Final Tech. Rep., 48 pp., U.S. Geol. Surv., Reston, Va.

Talwani, P. (1994), Ongoing Seismicity in the Vicinity of the Koyna and Warna Reservoirs, A Report to the United Nations Development Programme and Department of Science and Technology, Government of India, August, 85 pp.

Talwani, P. (1995), Speculation on the causes of continuing seismicity near Koyna Reservoir, India, Pure Appl. Geophy., 145, 167–174.

Talwani, P. (1996), Kaiser effect and reservoir induced seismicity, EOS Trans. AGU, 77, F500.

Talwani, P. (1997a), On the nature of reservoir-induced seismicity, Pure Appl. Geophy., 150, 473-492.

Talwani, P. (1997b), Seismotectonics of the Koyna-Warna Area, India, Pure Appl. Geophy., 150, 511- 550.

Talwani, P. (2000), Seismogenic properties of the crust inferred from recent studies of reservoir-induced seismicity-Application to Koyna, Curr. Sci. 79, 1327-1333.

Talwani, P., Kumara Swamy, S.V., and Sawalwade, C.B. (1996), Koyna Revisited : The Reevaluation of Seismicity Data in the Koyna-Warna Area, 1963– 1995, Univ. South Carolina Tech. Report (Columbia, South Carolina) 343 pp.

Talwani, P., Cobb, J.S., Schaeffer, M.F., (1999), In situ measurements of hydraulic properties of a shear zone in northwestern South Carolina, J. Geophys. Res., 104, 14993–15003.

Talwani, P., Chen, L., and Gahalaut, K. (2007), Seismogenic Permeability, k_s, J.Geophys. Res., 112, B07309, doi:10.1029/2006JB004665.

Templeton, E.L., and Rice, J.R. (2008), Off-fault plasticity and earthquake rupture dynamics: 1. Dry materials or neglect of fluid pressure changes, J. Geophys. Res., 113, B09306, doi:10.1029/2007JB005529.

Viesca, R. C., Templeton, E.L., and Rice, J.R. (2008), Off-fault plasticity and earthquake rupture dynamics: 2. Effects of fluid saturation, J. Geophys. Res., 113, B09307, doi:10.1029/2007JB005530.

Appendix I

The following expression (A1) relates the increase of pore pressure due to compression (undrained response), $\Delta p_u(r)$, at a distance r from the reservoir and the change in the mean stress $\Delta\sigma_{kk}/3$ at the given distance r

$$\Delta p_u(r) = -B\Delta\sigma_{kk}/3 \qquad (A1)$$

where B is the Skempton's coefficient.

An estimate of the change in the mean stress can be obtained following the procedure in Ahlvin and Ulery (1962). For a uniform circular load, the authors tabulated the vertical, radial and transverse stresses at a given depth and radial distance d from its center using elliptic functions. Considering the radius R of the circular loaded area to be 1.25km, for an earthquake located at a depth z=4 km and a radial distance ρ=2 km (i.e., $r=(4^2+2^2)^{1/2}$~4.5km), we obtain σ_z=-0.09193p, σ_ρ=-0.009830p and σ_θ=0.006325p, where p is the surface contact pressure. Therefore, the mean stress at a distance of 5 km is

$$\Delta\sigma_{kk}/3 \sim -0.032p \qquad (A2)$$

The maximum water height in Koyna is ~70 m, providing a surface contact pressure p of about 700 kPa

$$p = \rho gh = 1000x9.8x70 \sim 700 \text{ kPa}$$

and, substituting p in (A2), a mean stress value of about -22.4 kPa.

Assuming B~0.7 for crystalline rocks (Talwani et al., 1999), substituting in (A1) we obtain

$$\Delta p_u(5\text{km}) \sim 16 \text{ kPa}$$

The undrained response is one order of magnitude less than the diffused pore pressure values calculated in this study.

Table 1a. Lake levels and episodes of M ≥ 5.0 events near Koyna Reservoir.

Previous H_{max} exceeded on Y M D	New H_{max} reached on Y M D	New H_{max} (m)	Δh (m)	Episode	Eq. #	Event Date Y M D	Magnitude	Days after exceeded H_{max}	Fault Mechanism	Causative fault
	61 07 11	624.68								
62 07 11	62 08 15	636.65								
63 07 09	63 08 14	654.10								
64 08 01	64 08 13	654.94								
65 07 22	65 07 22	655.16								
67 08 30	67 10 04	656.99	1.83	I	1	67 09 13	5.2	14	Strike-slip (Langston, 1981)	KRFZ
					2	67 12 10	6.3		Strike-slip (Talwani, 1997b)	Near the intersection of KRFZ and L1
					3	67 12 10	5.0			L1
					4	67 12 11	5.2			P1
					5	67 12 12	5.4		Normal (Langston and Franco-Spera, 1985)	L3
					6	67 12 12	5.0		Strike-slip (Rao et al., 1975)	KRFZ
					7	67 12 12	5.0			L4
					8	67 12 24	5.5			P1
					9	67 12 25	5.1			KRFZ
					10	68 10 28	5.4			KRFZ
73 09 02	73 09 27	657.98	0.99	II	11	73 10 17	5.1	45	Strike-slip? (Gupta et al., 1980) CFPS	L1
80 09 01	80 09 03	658.13	0.15	III	12	80 09 02	5.5	1		L5
					13	80 09 20	5.3	19	Normal (Dziewonski et al., 1988)	KRFZ/L7
94 09 02	94 09 02	658.2	~0.1			No EQ.				
02 09 07	02 09 07	658.3	~0.1			No EQ.				

Data compiled from Talwani et al. (1996); Talwani (2000); Gupta et al. (2002)

Table 1b. Lake levels and episodes of M ≥ 5.0 events near Warna Reservoir

Previous H_{max} exceeded on Y M D	New H_{max} reached on Y M D	New H_{max} (m)	Δh (m)	Episode	Eq.#	Event Date Y M D	Magnitude	Days after Exceeded H_{max}	Fault Mechanism	Causative fault
	85 08 01	581.30								
86 06 25	86 06 30	586.15								
87 07 08	87 07 09	588.50								
88 07 14	88 07 19	592.65								
89 07 05	89 07 24	601.50								
90 07 09	90 07 16	604.15								
91 07 15	91 07 28	609.06								
92 07 29	92 08 19	617.90								
93 07 03	93 08 04	621.80	3.9	IV	14	93 12 08	5.2	158	Normal (Talwani, 1997)	Patan or L5
					15	94 02 01	5.4	213	Normal (Talwani, 1994)	Patan
94 09 02	94 09 02	622.05	0.25			NO EQ				
98 08 28	98 09 28	625.85	3.8	V	16	00 03 12	5.2	562	Normal (Gupta et al., 2002)	L6 or Patan
					17	00 04 06	5.1		Normal (Gupta et al., 2002)	L6 or P1
00 09 11	00 10 16	626.30	0.45	VI	18	00 09 05	5.3			L5
03* 09 10 (est)	03 09 13	627.88	1.58	VII	19	05 03 14	5.2	551	Normal (Kumar et al., 2006)	L5

Data compiled from Talwani et al. (1996), Gupta et al. (2002, 2005) and Satyanarayana et al. (2005).

Table 2a: Distances from Koyna dam to Episodes I, II and III

	Earthquake # (Date)	Route followed	Depth, z (km)	Horizontal distance along fractures, x (km)	Hypocentral Distance, r (km)	**Representative r (km)**
Episode I	2 (67 12 10)	KRFZ	10.0 (Talwani et al., 1996)	2.7	10.4	5, 10
Episode II	11 (73 10 17)	KRFZ, L1	4.0 (Talwani et al., 1996)	6.3	7.5	5, 10
Episode III	12 (80 09 02)	KRFZ, L5	8.0 (Gupta et al., 2000)	29.4	30.5	30
	13 (80 09 20)	KRFZ	12.0 (Gupta et al., 2000)	28.8	31.2	

Table 2b: Distances from Koyna dam to Episodes IV and V

	Earthquake # (Date)	Route followed	Depth, z (km)	Horizontal distance along fractures, x (km)	Hypocentral Distance, r (km)	**Representative r (km)**
Episode IV	14 (93 12 08)	KRFZ, L4 and Patan	8.2 (Talwani et al., 1996)	27.3	28.5	30
	15 (94 02 01)	KRFZ, L3 and Patan	8.8 (Talwani et al., 1996)	7.4	11.5	15
Episode V	16 (00 03 12)	KRFZ and L6	5.0 (Gupta et al., 2000)	28.2	28.6	30
	17 (00 04 06)	KRFZ and L6	7.8 (Gupta et al., 2000)	30.3	31.3	
Episode VI	18 (00 09 05)	KRFZ and L5	6.9 (Gupta et al., 2000)	28.2	29.0	30

Table 2c: Distances from Warna dam to Episodes IV and V

	Earthquake # (Date)	Route followed	Depth, z (km)	Horizontal distance along fractures, x (km)	Hypocentral Distance, r (km)	**Representative r (km)**
Episode IV	14 (93 12 08)	Lake, L4 and Patan	8.2 (Talwani et al., 1996)	15.0	17.1	15
	15 (94 02 01)	L3 and Patan	8.8 (Talwani et al., 1996)	25.0	26.5	30
Episode V	16 (00 03 12)	Lake, L4, P1 and L6	5.0 (Gupta et al., 2000)	20.0	20.6	20
	17 (00 04 06)	Lake, L4, P1 and L6	7.8 (Gupta et al., 2000)	17.7	19.3	
Episode VI	18 (00 09 05)	Lake, L4, P1 and L5	6.9 (Gupta et al., 2000)	16.0	17.4	15

Table 3a: Calculated values of pore pressure, p, for Episodes I, II and III, associated with lake level changes in the Koyna Reservoir.

	Episode I		Episode II				Episode III	
	p from start of impoundment		p from start of impoundment		p after Episode I		p from start of impoundment	p after Episode II
	p (r=5km)	p (r=10km)	p (r=5km)	p (r=10km)	p (r=5km)	p (r=10km)	p (r=30km)	p (r=30 km)
c=1 m2/s	450 kPa	320 kPa	410 kPa	340 kPa	380 kPa	270 kPa	200 kPa	90 kPa
c=5 m2/s	560 kPa	470 kPa	540 kPa	430 kPa	530 kPa	400 kPa	380 kPa	290 kPa
c=10 m2/s	590 kPa	520 kPa	580 kPa	490 kPa	580 kPa	470 kPa	420 kPa	360 kPa

Table 3b: Calculated values of pore pressure, p, for Episodes IV, V and VI, associated with lake level changes in the Koyna Reservoir.

	KOYNA							
	Episode IV				Episode V		Episode VI	
	p from start of impoundment		p after Ep. III		p from start of impoundment	p after Ep. IV	p from start of impoundment	p after Ep. V
	p (r=15km)	p (r=30km)	p (r=15km)	p (r=30km)	p (r=30km)	p (r=30km)	p (r=30km)	p (r=30km)
c=1m2/s	410 kPa	280 kPa	340 kPa	170 kPa	300 kPa	70 kPa	300 kPa	0.026 Pa
c=5m2/s	510 kPa	420 kPa	480 kPa	360 kPa	450 kPa	290 kPa	450 kPa	4 kPa
c=10m2/s	540 kPa	460 kPa	530 kPa	420 kPa	490 kPa	380 kPa	490 kPa	30 kPa

Table 3c: Calculated values of pore pressure, p, for Episodes IV, V and VI, associated with lake level changes in the Warna Reservoir.

	WARNA					
	Episode IV		Episode V		Episode VI	
	p from start of impoundment		p from start of impoundment	p after Ep. IV	p from start of impoundment	p after Ep. V
	p (r=15km)	p (r=30km)	p (r=20km)	p (r=20km)	p (r=15km)	p (r=15km)
c=1m2/s	160 kPa	50 kPa	210 kPa	140 kPa	280 kPa	1 kPa
c=5m2/s	290 kPa	180 kPa	370 kPa	330 kPa	380 kPa	70 kPa
c=10m2/s	350 kPa	240 kPa	420 kPa	390 kPa	400 kPa	140 kPa

Table 4a: Comparison of factors contributing to the generation of M≥5 earthquakes

	Year of filling cycle	Water level exceeds Hmax. (Evidence of Stress Memory)		ΔH (m)		A for c=5m2/s at 10 km distance (kPa/day)		M≥5	p (kPa)	
									Minimum value with leakage	Maximum value without leakage
Koyna	6/1967- 5/1968	Yes		36.11		1.48		Yes, Episode I.	-------	560
	6/1973-5/1974	Yes		47.09		1.90		Yes, Episode II.	400	540
	6/1975-5/1976	No		46.18		1.9		No	130	380
	6/1979-5/1980	No		45.41		2.24		No	280	420
	6/1980-5/1981	Yes		36.96		1.48		Yes, Episode III	290	420
Koyna + Warna		**Koyna**	**Warna**	**Koyna**	**Warna**	**Koyna**	**Warna**			
	6/1992-5/1993	No	No	43.90	32.60	1.98	1.30	No	620	780
	6/1993-5/1994	No	Yes	36.15	44.11	1.56	1.85	Yes, Episode IV	(eq. 14) 650 (eq. 15) 660	810 780
	6/1994-5/1995	Yes	Yes	36.00	41.88	1.62	1.90	No	160	860
	6/1995-5/1996	No	No	36.70	40.46	1.64	1.75	No	310	840
	6/1997-5/1998	No	No	23.25	40.15	1.62	1.70	No	480	880
	6/1998-5/1999	No	Yes	30.80	45.04	0.98	1.85	No	540	900
	6/1999-5/2000	No	No	22.40	33.77	0.96	1.40	Yes, Episode V	620	910
	6/2000-5/2001	No	Yes	22.50	38.09	1.02	1.60	Yes, Episode VI	74?	890

Table 4b: Comparison of filling rates, duration of high water levels and episodes

		Koyna		Warna	
Filling cycle	**Episode**	**Filling rate (m/day)**	**Duration water level >651m (days)**	**Filling rate (m/day)**	**Duration water level >615m (days)**
1967-1968	I	0.95	173		
1973-1974	II	0.52	142		
1975-1976		0.58	155		
1979-1980		0.89	153		
1980-1981	III	0.76	128		
1992-1993		0.73	120	0.56	52
1993-1994	IV	0.53	168	0.83	148
1994-1995		0.83	143	0.77	165
1995-1996		0.47	127	0.53	158
1997-1998		0.48	163	0.88	146
1998-1999		0.30	168	0.46	205
1999-2000	V	0.82	190	0.34	215
2000-2001	VI	0.23	112	0.36	

Table 5: Comparison of triggering factors

	Evidence of stress memory		**ΔH > 40 m**		**A > 1.8 kPa/day**		**Filling rate >0.75 m/day**		**Duration > 160 days**	
	Observed		**Observed**		**Observed**		**Observed**		**Observed**	
	Yes	No	Yes	No	Yes	No	Yes	No	Yes	No
Episode	5	1	2	4	2	4	4	2	3	3
No episode	2		7		5		4		4	

.

Figure Captions.

Figure 1a: Koyna and Warna water level fluctuations from impoundment to 2001, and daily histogram of the number of M≥4.0 recorded earthquakes (catalog from Gupta, 2000).

Figure 1b: Koyna and Warna water level fluctuations from impoundment to 2001, and times of occurrence of M≥5.0 earthquakes (Episodes I to VI).

Figure 2: Location of Koyna-Warna region in western India, (inset), showing the chronological locations of 19 M≥5 events, taken from Talwani et al.(1996), Gupta et al.(2002 and 2005) superposed on the revised seismotectonic framework (this study) modified from Talwani (1997a) (See text for details). D is the Donachiwada fault, with fissures associated with the 1967 shock.

Figure 3: Temporal distribution of M ≥5 events and the seven episodes of stress memory, compared with the lake levels. The solid dots show the date when the previous maximum water level was exceeded, and the horizontal bars when it was not. The initial fillings of the Koyna and Warna Reservoirs (1961-1965 and 1985-1992) were followed by small rises in those two reservoirs (shown with an exaggerated scale). M≥5 events, constituting the episodes were found to occur only when the previous lake level was exceeded, displaying stress memory in the rocks of the KWR.

Figure 4a: Effect of maintaining a constant level of water above pre-impoundment levels, calculated for a six year period. The pore pressures (shown in red crosses) have been normalized with respect to the lake levels.

Figure 4b: Effect of six loading and unloading 1year-cycles (blue) on the diffused pore pressure (red). The pore pressures have been normalized with respect to the lake levels.

Figure 5: The top panel shows the water levels in Koyna Reservoir from the beginning of impoundment in 1961 to 1990. The middle panel shows the calculated build up of diffused pore pressure for c=1 m^2/s at different distances (5km, 10km, 15km, 20km), and the times of Episodes I, II and III. The accumulated pore pressures on 1/1/1990 for various distances are given for each curve in kPa. The bottom panel shows the daily rate of pore pressure change in Pa/day.

Figure 6: Build up of diffused pore pressures from beginning of impoundment of Koyna Reservoir to the time of the main shock in 1967 (earthquake # 2) at distances of 5 and 10 km for different values of c (middle and bottom panels). The pore pressures are compared with the daily water level (top panels).

Figure 7: The top panel shows the water levels in Koyna Reservoir from the beginning of impoundment in 1961 to 1990. The middle panel shows the calculated build up of diffused pore pressure for c=5 m^2/s at different distances (5km, 10km, 15km, 20km, 30km), and the times of Episodes I, II and III. The accumulated pore pressures on 1/1/1990 for various distances are given for each curve in kPa. The bottom panel shows the daily rate of pore pressure change in Pa/day. In the curve showing dp/dt, the horizontal ticks define the amplitude of annual dp/dt increase (A) for the 1973 cycle (Pa/day) for c=5m^2/s and r=10km, i.e. 1900 Pa/day. A is listed in Table 4a for various filling cycles.

Figure 8: Build up of diffused pore pressure from Koyna Reservoir at a distances of 5 and 10 km, assuming complete leakage of pore pressure during Episode I. Pore pressures are calculated for different values of c after the end of Episode I (earthquake # 10) up to the beginning of Episode II (earthquake # 11).

Figure 9: Build up of diffused pore pressure from Koyna Reservoir at a distance of 30 km, assuming complete leakage of pore pressure during Episode II. Pore pressures are calculated for different values of c from the end of Episode II (earthquake # 11) to the beginning of Episode III (earthquake # 12).

Figure 10: The top panel shows the water levels in Warna Reservoir from the beginning of impoundment in 1985 to 2000. The middle panel shows the calculated build up of diffused pore pressure for $c=5m^2/s$ at different distances (10km, 15km, 20km), and the times of Episode IV, V and VI. The accumulated pore pressures on 1/1/1990 for various distances are given for each curve in kPa. The bottom panel shows the daily rate of pore pressure change in Pa/day.

Figure 11: The top panel shows the water levels in Warna Reservoir from the beginning of impoundment in 1985 to 2000. The middle panel shows the calculated build up of diffused pore pressure for $c=10m^2/s$ at different distances (10km, 15km, 20km) and the times of Episode IV, V and VI. The accumulated pore pressures on 1/1/1990 for various distances are given for each curve in kPa. The bottom panel shows the rate of pore pressure change in Pa/day.

Figure 12: Build up of diffused pore pressure from Warna Reservoir at a distance of 15 km from the beginning of impoundment to the beginning of Episode IV (earthquake # 14).

Figure 13: Build up of diffused pore pressure from Warna Reservoir at a distance of 20 km assuming complete leakage of pore pressure during Episode IV (earthquakes # 14 and # 15). Pore pressures are calculated from the end of Episode IV (earthquake # 15) to the beginning of Episode V (earthquake #16).

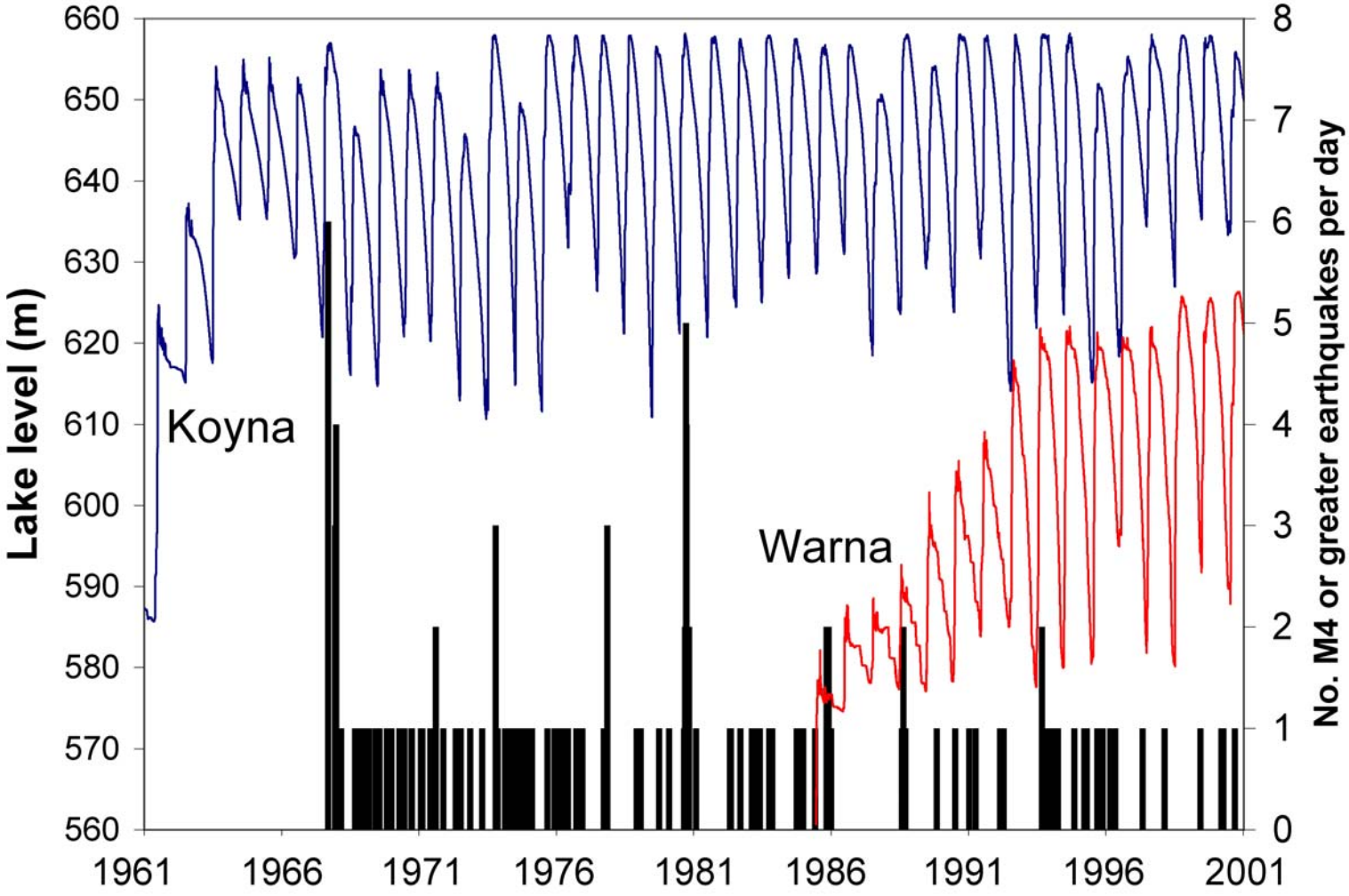

Figure 1a: Koyna and Warna water level fluctuations from impoundment to 2001, daily histogram of the number of M≥4.0 recorded earthquakes (catalog from Gupta, 2000).

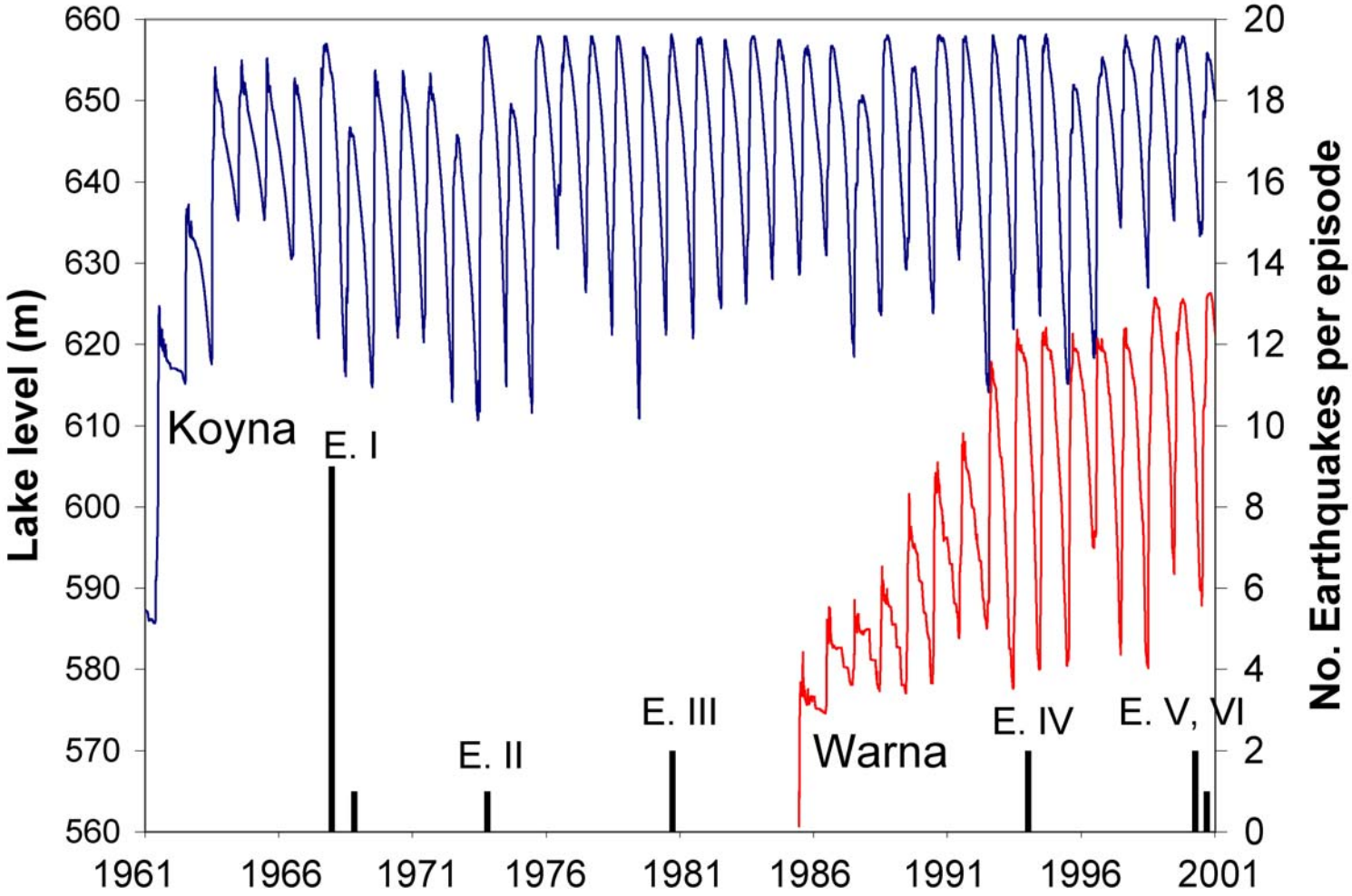

Figure 1b: Koyna and Warna water level fluctuations from impoundment to 2001, and times of occurrence of M≥5.0 earthquakes (Episodes I to V).

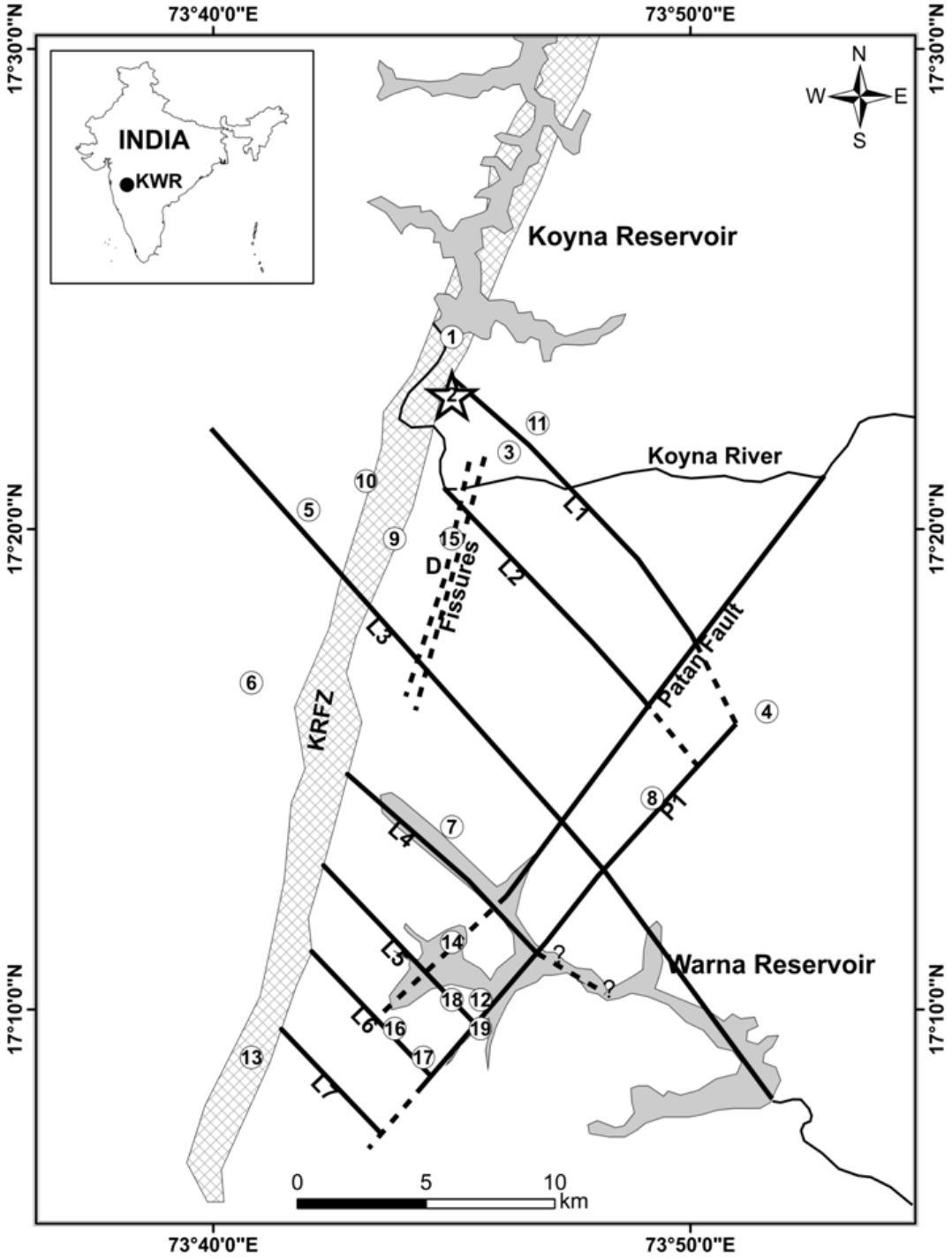

Figure 2: Location of Koyna-Warna region in western India, (inset), showing the chronological locations of 19 M≥5 events, taken from Talwani et al.(1996), Gupta et al.(2002 and 2005) superposed on the revised seismotectonic framework (this study) modified from Talwani (1997a) (See text for details). D is the Donachiwada fault, with fissures associated with the 1967 shock.

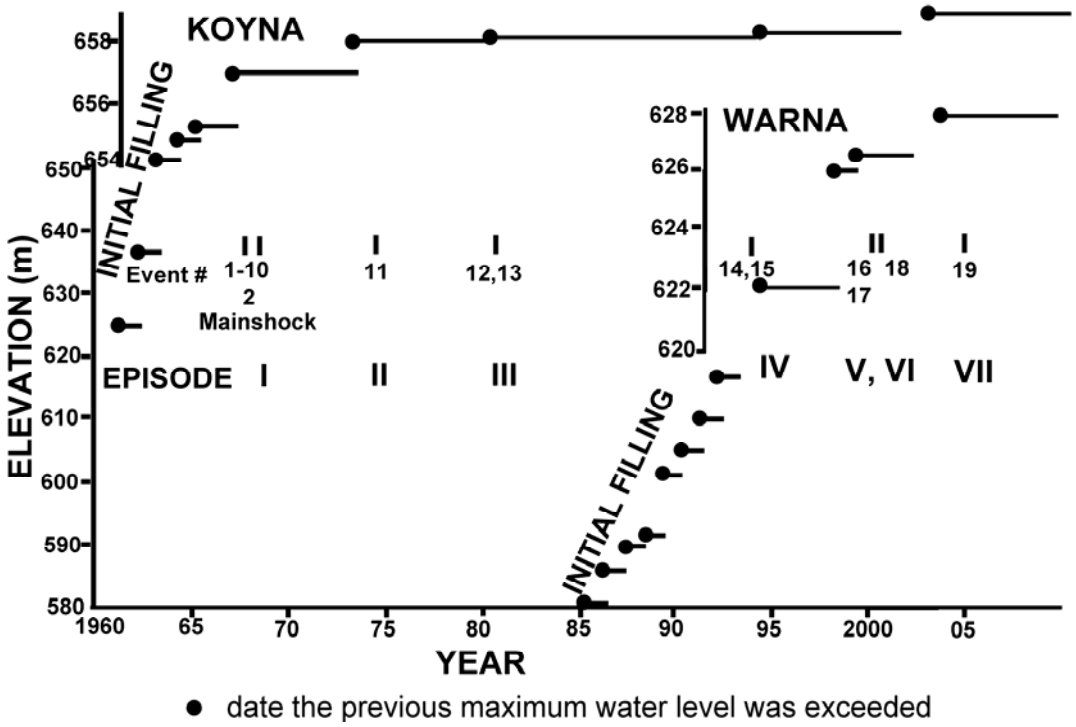

Figure 3: Temporal distribution of M ≥5 events and the seven episodes of stress memory, compared with the lake levels. The solid dots show the date when the previous maximum water level was exceeded, and the horizontal bars when it was not. The initial fillings of the Koyna and Warna Reservoirs (1961-1965 and 1985-1992) were followed by small rises in those two reservoirs (shown with an exaggerated scale). M≥5 events, constituting the episodes were found to occur only when the previous lake level was exceeded, displaying stress memory in the rocks of the KWR.

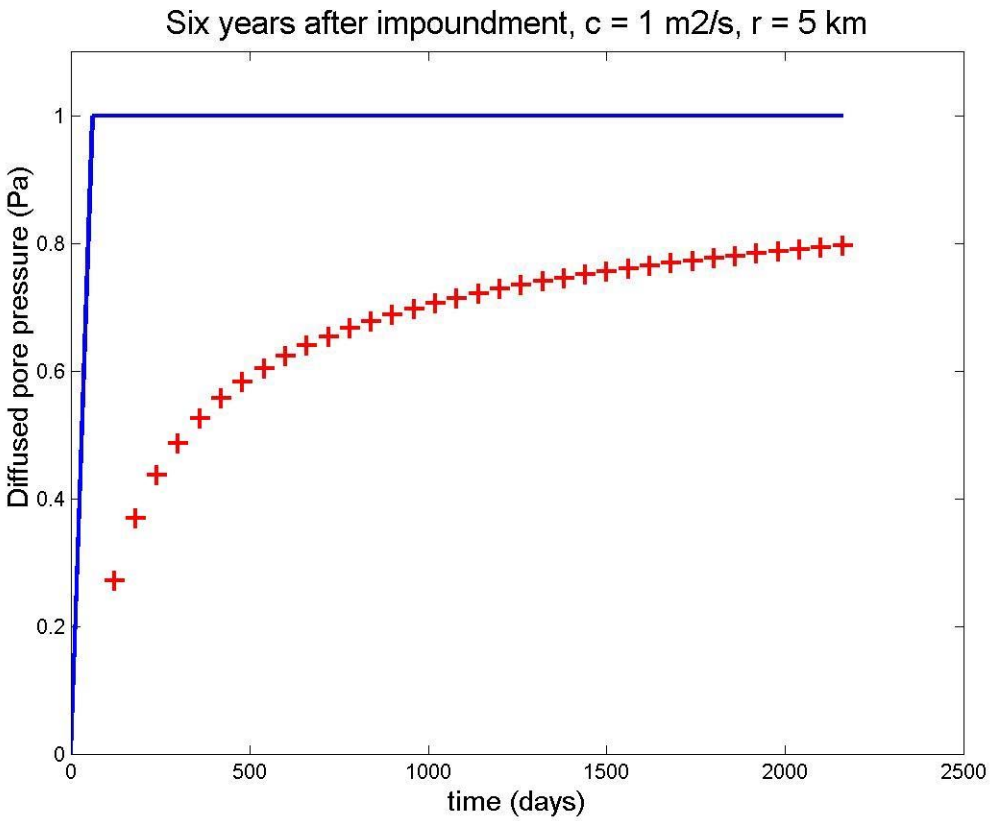

Figure 4a: Effect of maintaining a constant level of water above pre-impoundment levels, calculated for a six year period. The pore pressures (shown in red crosses) have been normalized with respect to the lake levels.

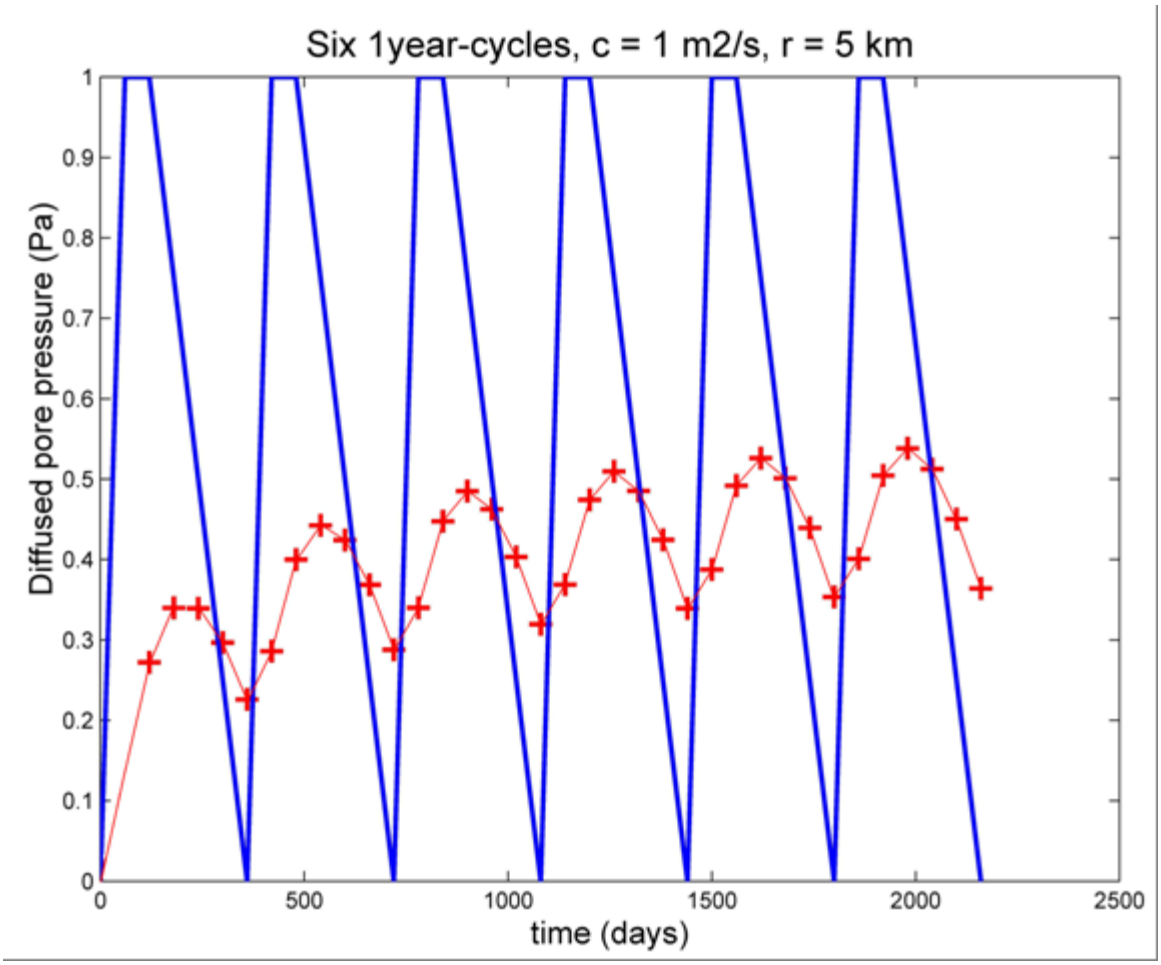

Figure 4b: Effect of six loading and unloading 1year-cycles (blue) on the diffused pore pressure (red). The pore pressures have been normalized with respect to the lake levels.

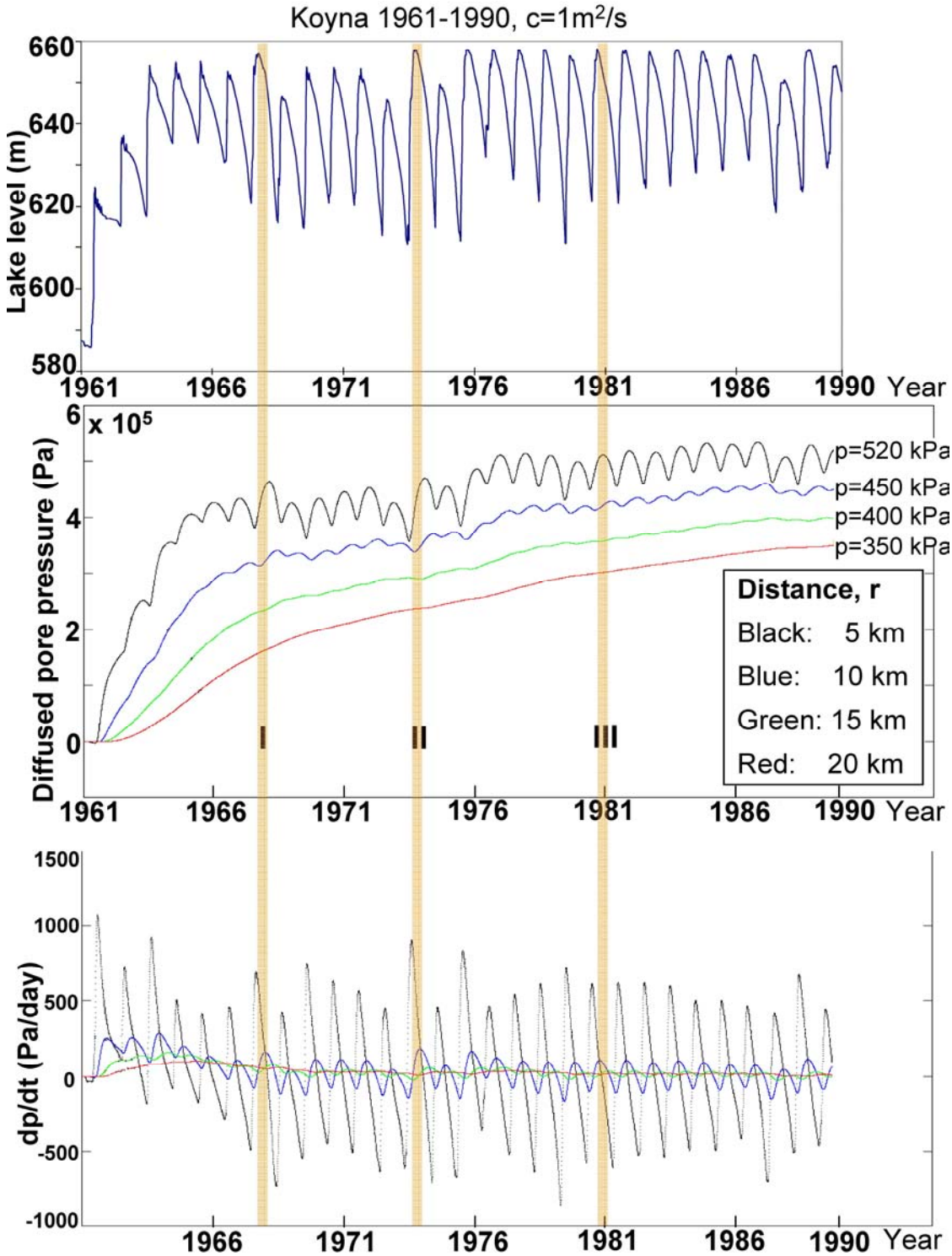

Figure 5: The top panel shows the water levels in Koyna Reservoir from the beginning of impoundment in 1961 to 1990. The middle panel shows the calculated build up of diffused pore pressure for c=1 m^2/s at different distances (5km, 10km, 15km, 20km), and the times of Episodes I, II and III. The accumulated pore pressures on 1/1/1990 for various distances are given for each curve in kPa. The bottom panel shows the daily rate of pore pressure change in Pa/day.

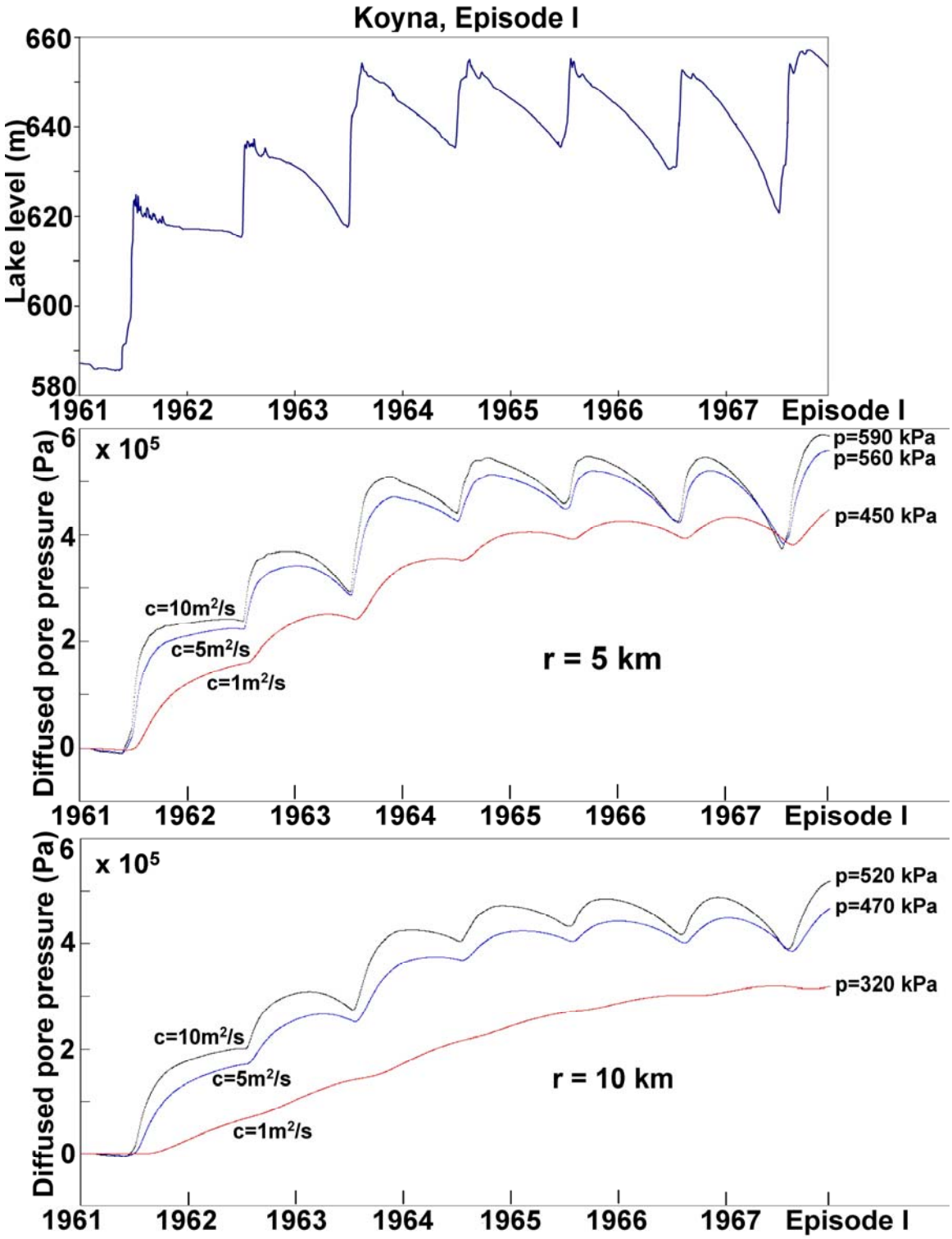

Figure 6: Build up of diffused pore pressures from beginning of impoundment of Koyna Reservoir to the time of the main shock in 1967 (earthquake # 2) at distances of 5 and 10 km for different values of c (middle bottom panels). The pore pressures are compared with the daily water level (top panel).

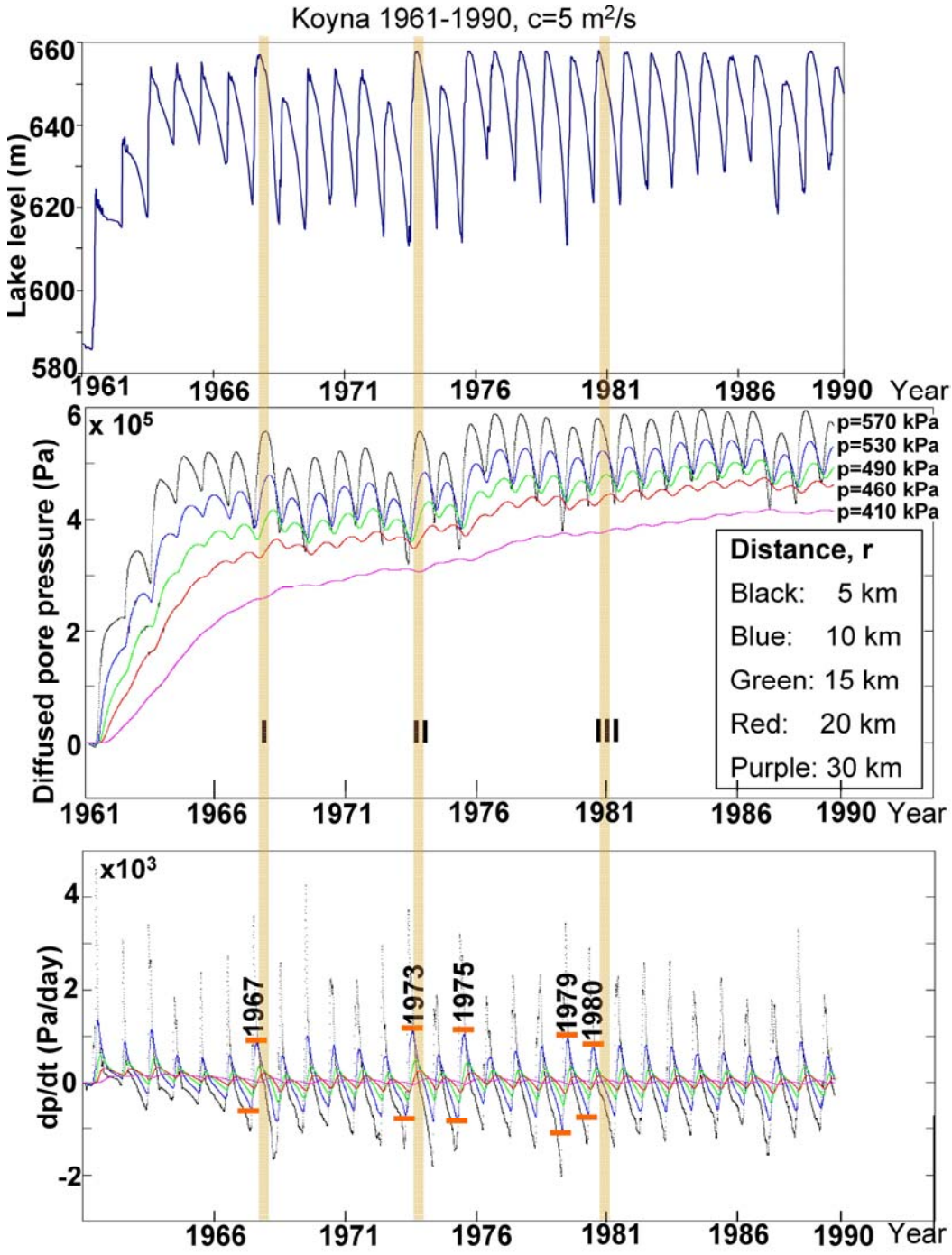

Figure 7: The top panel shows the water levels in Koyna Reservoir from the beginning of impoundment in 1961 to 1990. The middle panel shows the calculated build up of diffused pore pressure for c=5 m^2/s at different distances (5km, 10km, 15km, 20km, 30km), and the times of Episodes I, II and III. The accumulated pore pressures on 1/1/1990 for various distances are given for each curve in kPa. The bottom panel shows the daily rate of pore pressure change in Pa/day. In the curve showing dp/dt (Pa/day), the horizontal ticks define the amplitude of annual dp/dt increase (A), for c=5m^2/s and r=10km, associated with each episode. E.g. for Episode II (1973 filling cycle), A=1900 Pa/day. A is listed on Table 4 for various filling cycles.

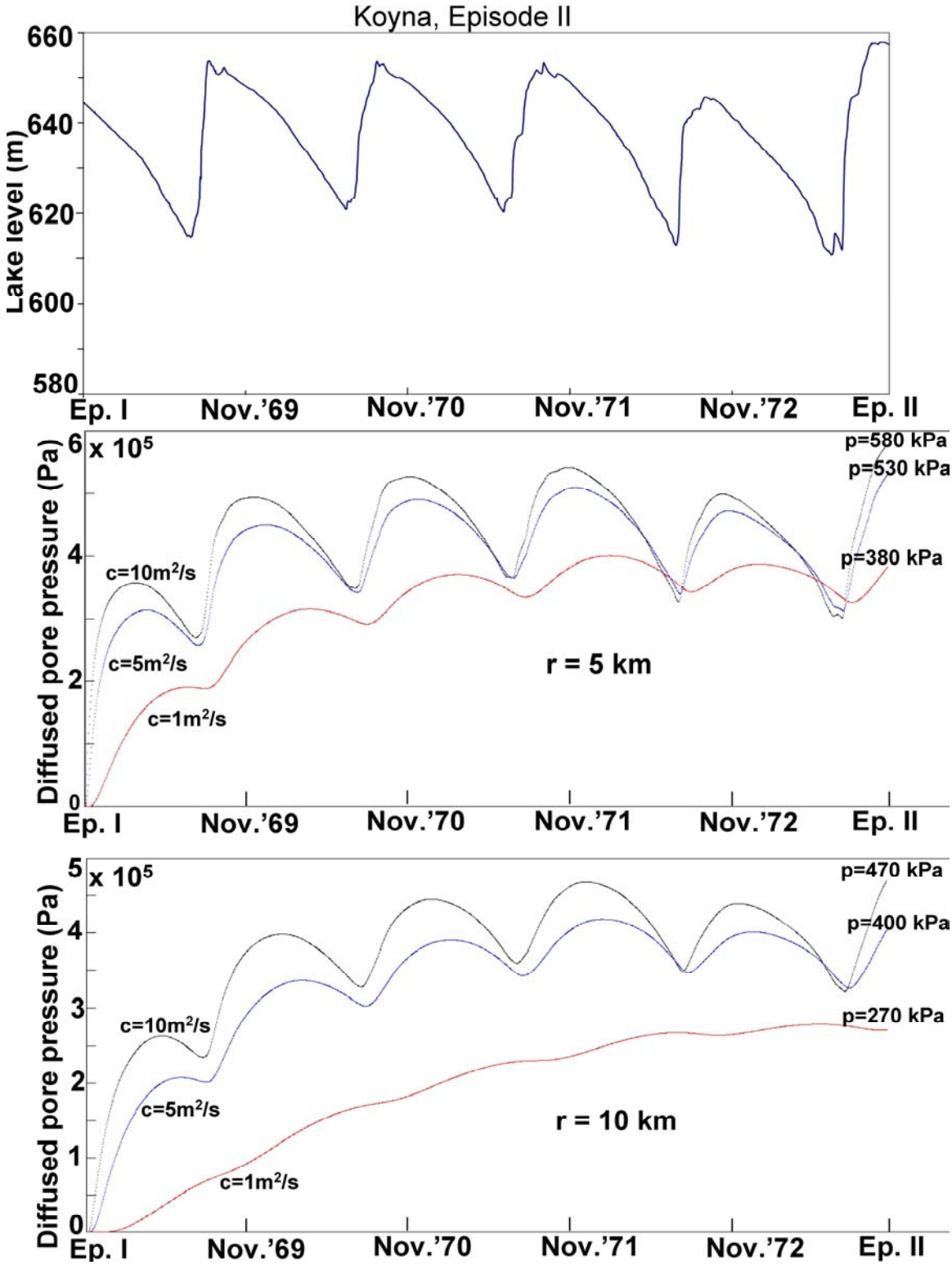

Figure 8: Build up of diffused pore pressure from Koyna Reservoir at a distances of 5 and 10 km, assuming complete leakage of pore pressure during Episode I. Pore pressures are calculated for different values of c after the end of Episode I (earthquake # 10) up to the beginning of Episode II (earthquake # 11).

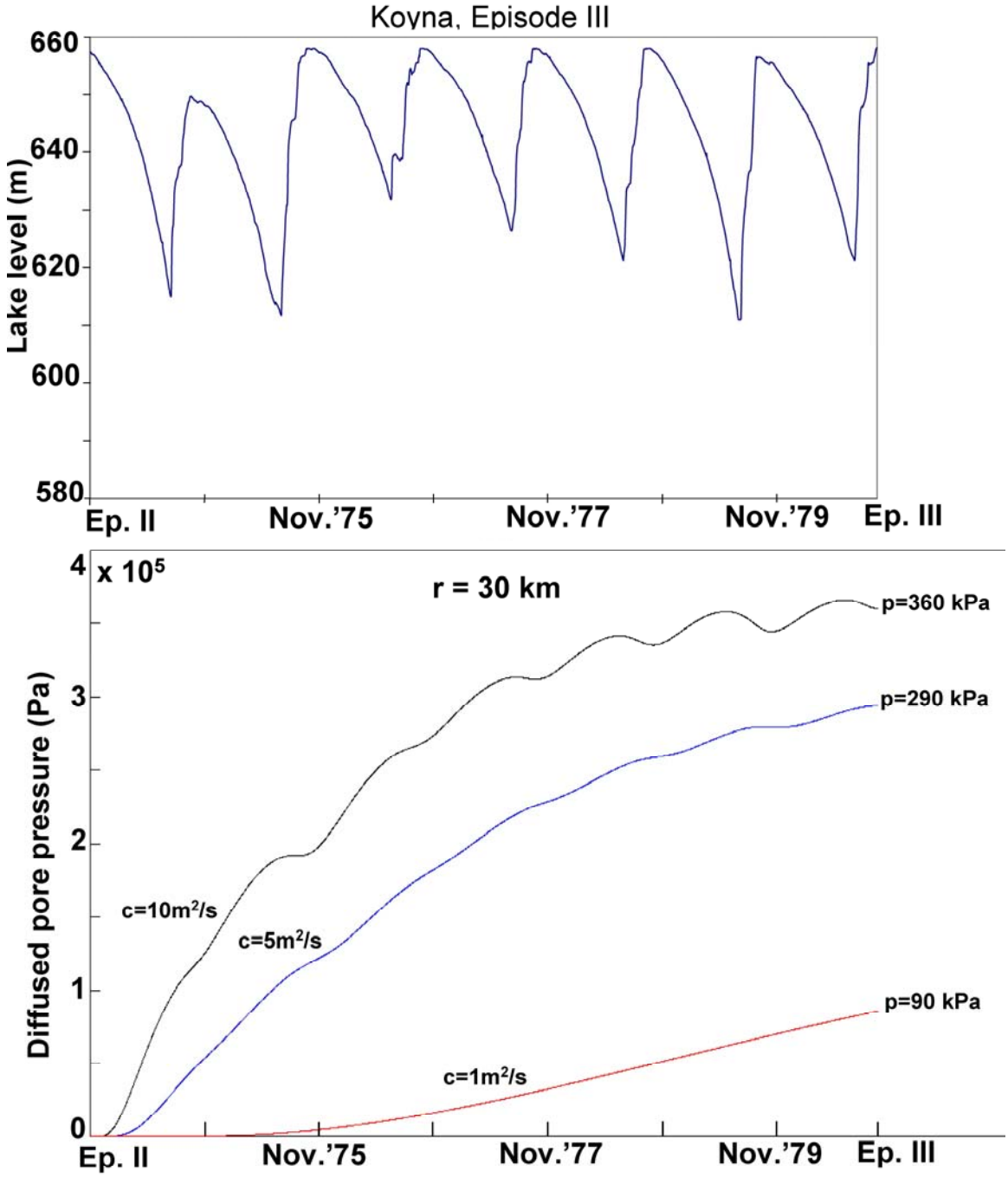

Figure 9: Build up of diffused pore pressure from Koyna Reservoir at a distance of 30 km, assuming complete leakage of pore pressure during Episode II. Pore pressures are calculated for different values of c from the end of Episode II (earthquake # 11) to the beginning of Episode III (earthquake # 12).

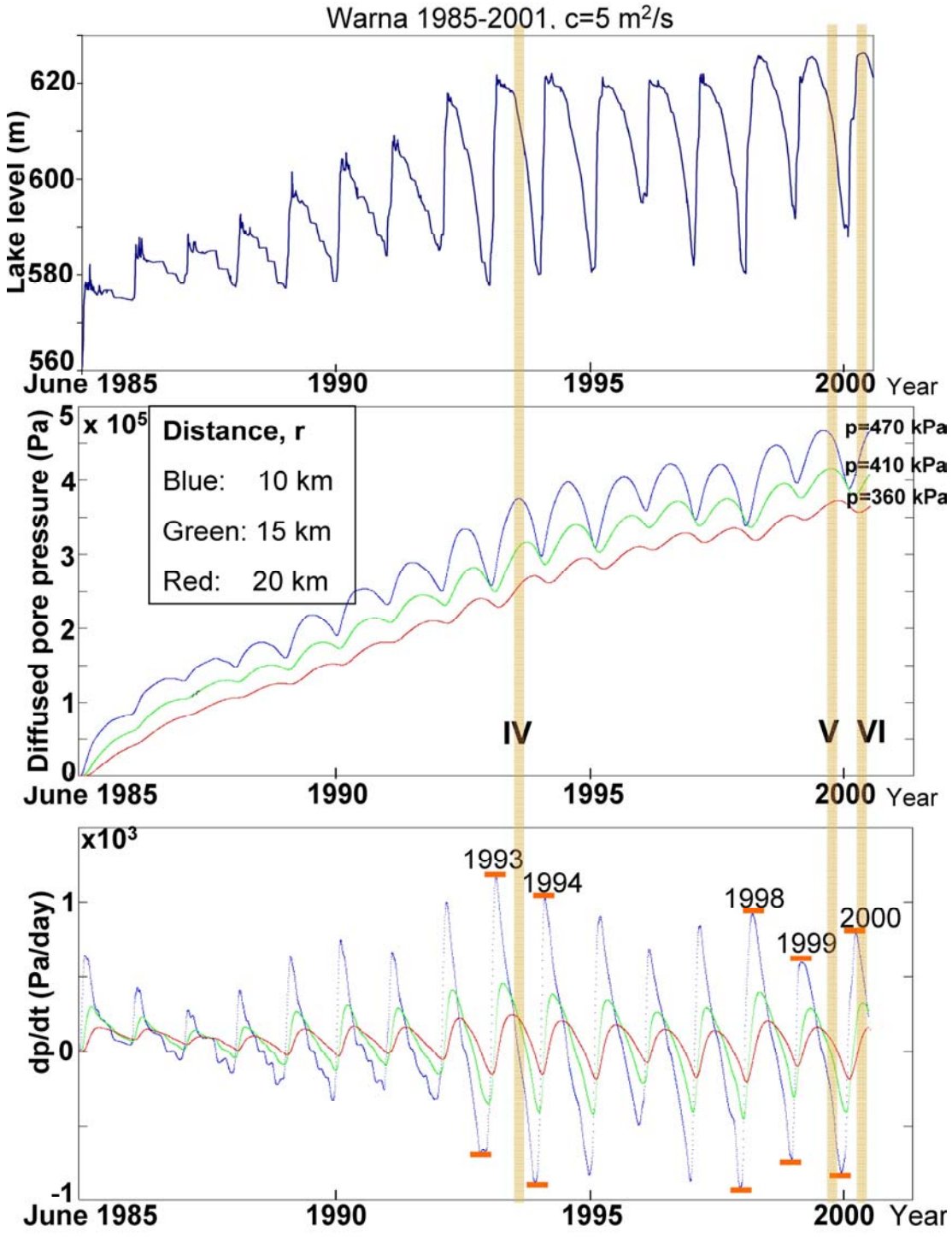

Figure 10: The top panel shows the water levels in Warna Reservoir from the beginning of impoundment in 1985 to 2000. The middle panel shows the calculated build up of diffused pore pressure for c=5m^2/s at different distances (10km, 15km, 20km), and the times of Episode IV, V and VI. The accumulated pore pressures on 1/1/1990 for various distances are given for each curve in kPa. The bottom panel shows the daily rate of pore pressure change in Pa/day.

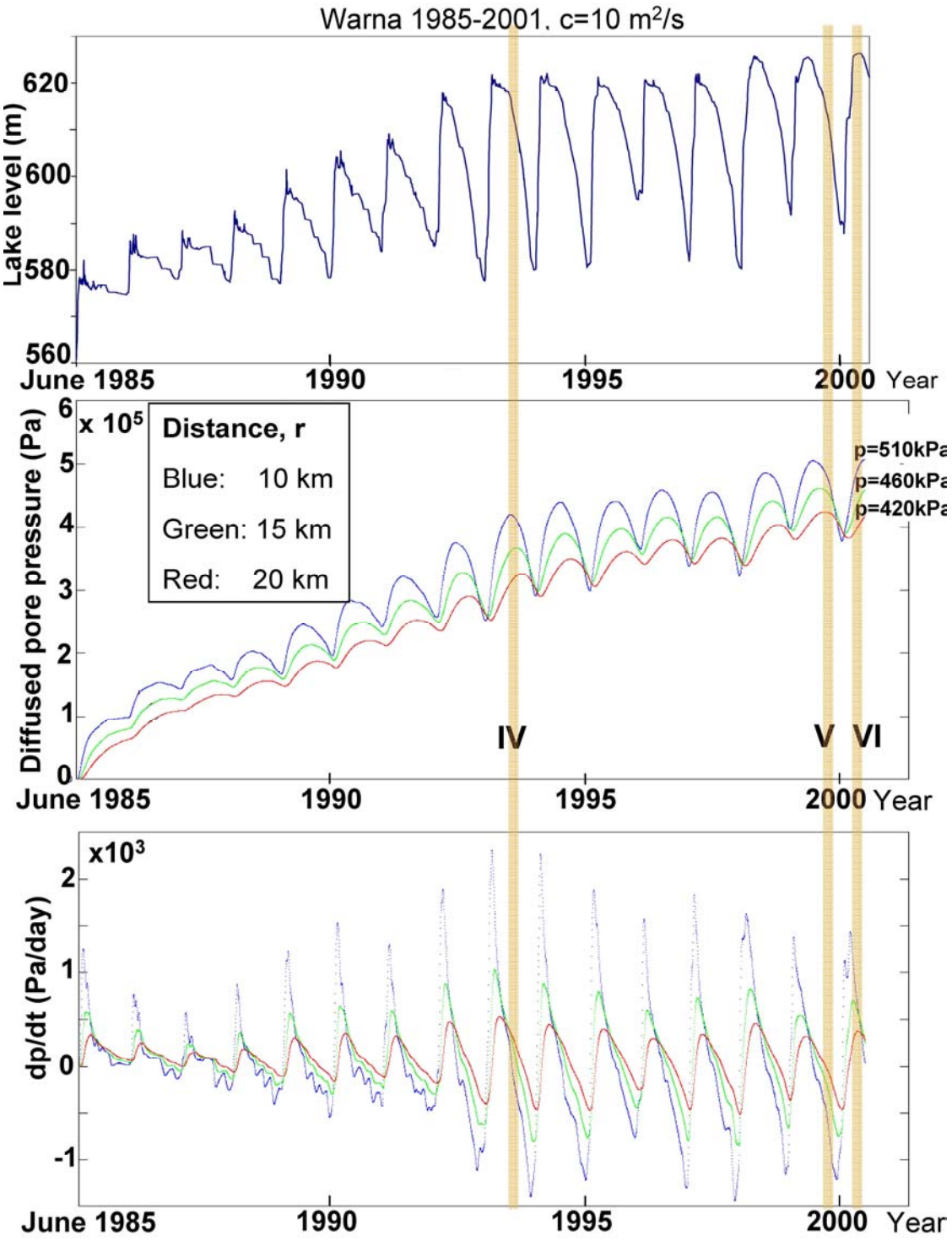

Figure 11: The top panel shows the water levels in Warna Reservoir from the beginning of impoundment in 1985 to 2000. The middle panel shows the calculated build up of diffused pore pressure for c=10m^2/s at different distances (10km, 15km, 20km) and the times of Episode IV, V and VI. The accumulated pore pressures on 1/1/1990 for various distances are given for each curve in kPa. The bottom panel shows the rate of pore pressure change in Pa/day.

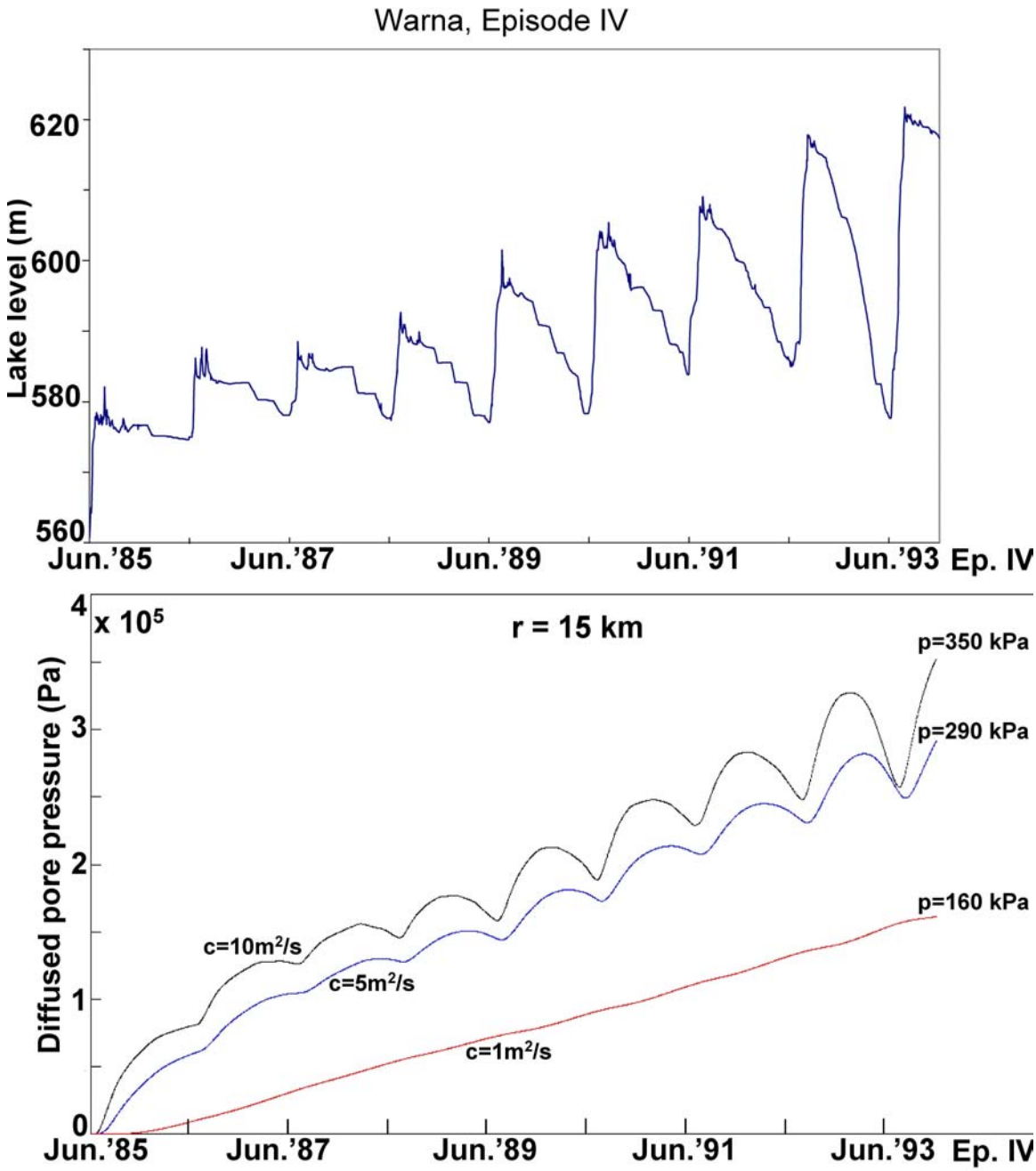

Figure 12: Build up of diffused pore pressure from Warna Reservoir at a distance of 15 km from the beginning of impoundment to the beginning of Episode IV (earthquake # 14).

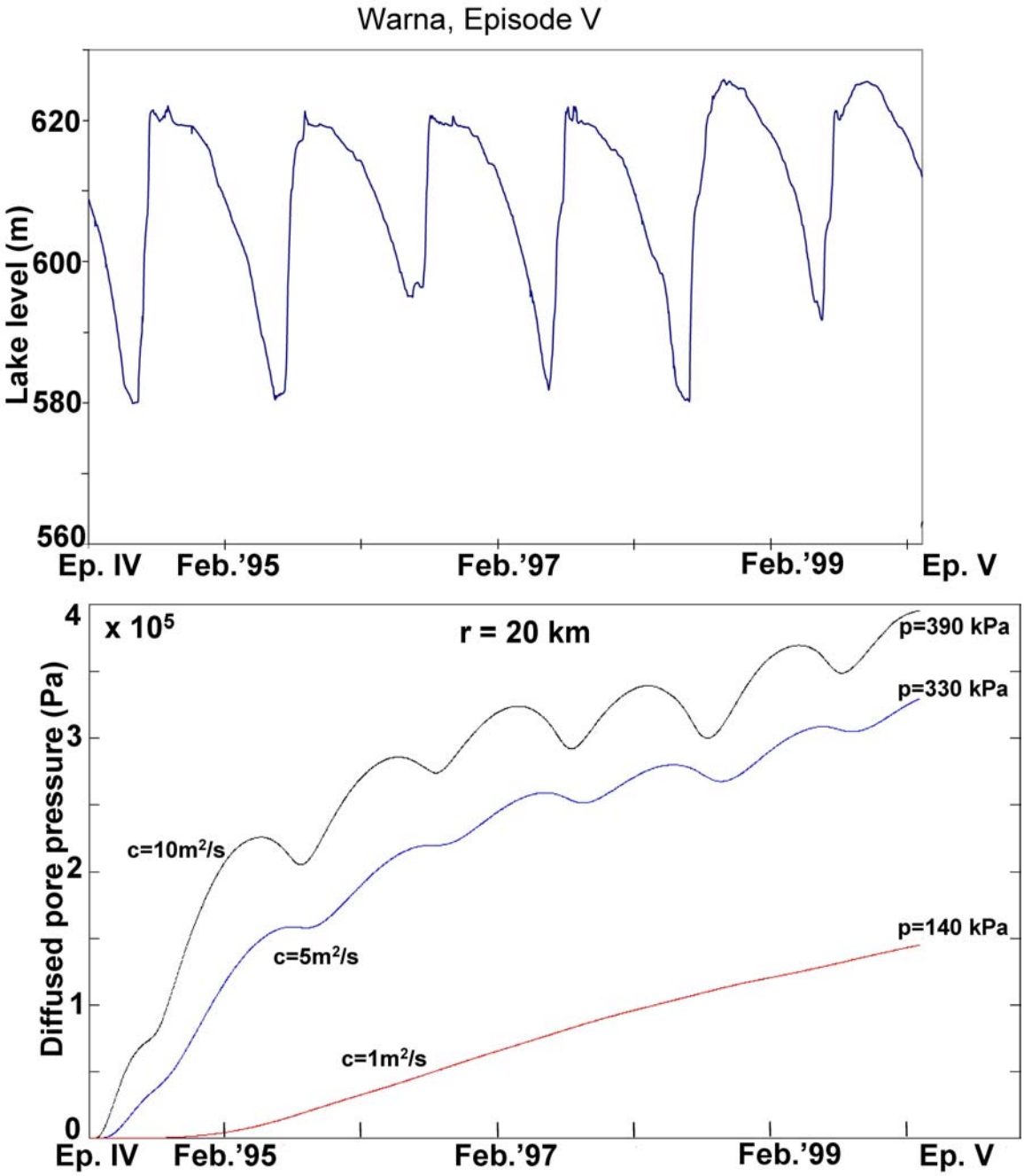

Figure 13: Build up of diffused pore pressure from Warna Reservoir at a distance of 20 km assuming complete leakage of pore pressure during Episode IV (earthquakes # 14 and # 15). Pore pressures are calculated from the end of Episode IV (earthquake # 15) to the beginning of Episode V (earthquake # 16).